Atmos. Chem. Phys., 11, 8635–8659, 2011
www.atmos-chem-phys.net/11/8635/2011/
doi:10.5194/acp-11-8635-2011

Atmospheric Chemistry and Physics

Estimating the direct and indirect effects of secondary organic aerosols using ECHAM5-HAM

D. O'Donnell[1,*], **K. Tsigaridis**[2,**], **and J. Feichter**[1,*]

[1]Max Planck Institute for Meteorology, Bundesstrasse 55, 20146 Hamburg, Germany
[2]Laboratoire des Sciences du Climat et de l'Environnement (LSCE), 91191 Gif-sur-Yvette, France
[*]now at: Institute for Atmospheric Science and Climate, ETH Zürich, Universitätstrasse 16, 8092 Zürich, Switzerland
[**]now at: Center for Climate System Research, Columbia University and NASA Goddard Institute for Space Studies, 2880 Broadway, New York NY10025, USA

Received: 20 December 2010 – Published in Atmos. Chem. Phys. Discuss.: 24 January 2011
Revised: 14 June 2011 – Accepted: 10 August 2011 – Published: 25 August 2011

Abstract. Secondary organic aerosol (SOA) has been introduced into the global climate-aerosol model ECHAM5/HAM. The SOA module handles aerosols originating from both biogenic and anthropogenic sources. The model simulates the emission of precursor gases, their chemical conversion into condensable gases, the partitioning of semi-volatile condenable species into the gas and aerosol phases. As ECHAM5/HAM is a size-resolved model, a new method that permits the calculation of partitioning of semi-volatile species between different size classes is introduced. We compare results of modelled organic aerosol concentrations against measurements from extensive measurement networks in Europe and the United States, running the model with and without SOA. We also compare modelled aerosol optical depth against measurements from the AERONET network of grond stations. We find that SOA improves agreement between model and measurements in both organic aerosol mass and aerosol optical depth, but does not fully correct the low bias that is present in the model for both of these quantities. Although many models now include SOA, any overall estimate of the direct and indirect effects of these aerosols is still lacking. This paper makes a first step in that direction. The model is applied to estimate the direct and indirect effects of SOA under simulated year 2000 conditions. The modelled SOA spatial distribution indicates that SOA is likely to be an important source of free and upper tropospheric aerosol. We find a negative shortwave (SW) forcing from the direct effect, amounting to $-0.31\,\mathrm{Wm}^{-2}$ on the global annual mean. In contrast, the model indicates a positive indirect effect of SOA of $+0.23\,\mathrm{Wm}^{-2}$, arising from the enlargement of particles due to condensation of SOA, together with an enhanced coagulation sink of small particles. In the longwave, model results are a direct effect of $+0.02\,\mathrm{Wm}^{-2}$ and an indirect effect of $-0.03\,\mathrm{Wm}^{-2}$.

Correspondence to: D. O'Donnell
(declan.odonnell@env.ethz.ch)

1 Introduction

Organic aerosols constitute an important part of the tropospheric aerosol loading. In regions affected by anthropogenic pollution, organic species have been observed to be the second most abundant component by mass after sulphate, and frequently the most important contributor to aerosol light scattering (Hegg et al., 1997; Novakov et al., 1997; Ramanathan et al., 2001). In tropical forested areas, it forms the dominant part of the aerosol mass (Andreae and Crutzen, 1997; Artaxo et al., 1988, 2002), even in the absence of large-scale biomass burning. Organic aerosols are found in the remote marine environments (Middlebrook et al., 1998), in the free troposphere (Huebert et al., 2004; Heald et al., 2005) and in the upper troposphere (Murphy et al., 1998; Froyd et al., 2009).

Organic aerosol may be formed by direct emission into the atmosphere (primary organic aerosols, POA) or by the atmospheric oxidation of a gas-phase precursor (secondary organic aerosol, SOA). Most models (including ECHAM5-HAM) take POA to be composed of non-volatile substances that exist only in the particulate phase, although recent works (Robinson et al., 2007; Pye and Seinfeld, 2010) have shown that it is in fact a mixture of many organic species whose saturation vapour pressure spans several orders of magnitude. Both biogenic and anthropogenic SOA precursors are known. Estimates of global emissions of the biogenic

precursors isoprene (600 Tg yr^{-1}, Guenther et al., 2006) and monoterpenes (140 Tg yr^{-1}, Guenther et al., 1995) indicate that biogenic emissions are are an order of magnitude greater than those of known anthropogenic precursors (17 Tg yr^{-1}, Olivier et al., 2005).

Furthermore, some measurements show a concentration of organic aerosol that is well above that predicted by the current generation of global aerosol-climate models (Heald et al., 2005; Volkamer et al., 2006). Most such models include only POA or include SOA in a very simple, implicit treatment, for example the AEROCOM approach (Dentener et al., 2006), in which SOA is considered to be formed in fixed proportion to prescribed monoterpene emissions in each grid box, and to have identical properties to (and therefore possible to lump together with) POA.

Explicit treatment of SOA in models has to date been performed mainly using atmospheric chemistry models and few have attempted to quantify the climate influence of such aerosols in isolation. Chung and Seinfeld (2002), considering only biogenic precursors, estimated a global annual mean SOA burden of 0.19 Tg from a production of 11.2 Tg yr^{-1}. Tsigaridis and Kanakidou (2003) included anthropogenic aromatic precursors (not including benzene, not known at that time to be a significant SOA precursor) in a sensitivity study that attempted to constrain the SOA production and atmospheric burden, estimating the production bounds to be 2.5–44.5 Tg yr^{-1}. These studies exclude isoprene, since they predate the discovery that isoprene can be a significant source of SOA. Henze and Seinfeld (2006) first included SOA from isoprene in a global study, with the result that SOA production almost doubled and the SOA burden more than doubled (to 16.4 Tg yr^{-1} and 0.39 Tg respectively) compared with the same model without SOA from isoprene. Hoyle et al. (2007), although using isoprene emissions lower than other models, estimated SOA production of 55–69 Tg yr^{-1} and a SOA burden of 0.52–0.70 Tg in the global annual mean. Hoyle et al. (2009), using an offline radiative transfer model, and assuming an external aerosol mixture, estimated the radiative forcing (present day minus preindustrial) of anthropogenic SOA to be -0.06–0.09 Wm^{-2}.

In this study, we examine how the aerosol direct effect and indirect effects are affected by secondary organic aerosols using the aerosol-climate model ECHAM5/HAM (Stier at al., 2005), which has been extended to handle SOA. This allows us to deploy a model with online radiation and cloud microphysics that are coupled to an aerosol population which is resolved in both aerosol size distribution and mixing state. Both particle size distribution and mixing state are important for the calculation of radiative properties, and at least the size distribution is important for aerosol indirect effects (Stier et al., 2005).

2 Model description

The model upon which this study is based is ECHAM5/HAM, described and evaluated in Stier et al. (2005), with cloud microphysics described in Lohmann et al. (2007). Here, only a brief synopsis of the main model features is given: for details, the reader is referred to the works cited above.

ECHAM5/HAM is a modal model that describes the aerosol population as a superposition of seven lognormal modes. For each mode, aerosol mass and number concentrations are prognostic variables. Four of these modes are termed "soluble", which means, in the context of this model, that the particles are internally mixed and may take up water. Soluble modes cover the size ranges 1–10 nm (nucleation mode), 10–100 nm (Aitken mode), 100 nm–1 µm (accumulation mode) and >1 µm (coarse mode) dry particle diameter. Insoluble modes do not take up water, are regarded as externally mixed and cover Aitken, accumulation and coarse modes. The modelled aerosol species are sulphate, black carbon, organic carbon, sea salt and mineral dust. In the original model version, "organic carbon" refers to POA plus SOA formed by assuming a fixed 15 % SOA yield from the monoterpene emissions estimates of Guenther et al. (1995), with immediate non-volatile SOA production in the emitting gridbox. This approach is no longer used. Modelled processes include emission, aerosol microphysics (water uptake, condensation of SO_4 from the gas phase, new particle nucleation, and coagulation), sink processes (wet deposition, dry deposition and sedimentation), aerosol radiative effects and cloud droplet activation. Aersol optical depth is calculated for each mode (except the nucleation mode) as a function of aersol number, aerosol wet radius and the complex refractive index (obtained as a volume-weighted contribution of each of the aerosol species in the mode). Cloud droplet number concentration (CDNC) and ice crystal number concentration (ICNC) are calculated as functions of the aerosol size distribution and possibly composition, depending on the activation scheme chosen. The model includes a simple sulphate chemistry scheme, for which prescribed monthly mean oxidant concentrations with a superimposed diurnal cycle are used.

A SOA scheme, described in the following subchapters, has been added to this model. The aim is to keep this scheme as simple and computationally cost-effective as possible while capturing the most significant known SOA sources. The model with SOA takes approximately 35 % more CPU time than ECHAM5/HAM without SOA.

2.1 Emission of SOA precursors

Precursor species included in the model are isoprene and monoterpenes, which are emitted by vegetation, and selected aromatic compounds, detailed below, which are anthropogenic.

Emission of biogenic species is calculated online in the model using MEGAN (Guenther et al., 2006; Guenther, 2007) for isoprene and the earlier work of (Guenther et al., 1995) for monoterpenes. No distinction is made between different monoterpene species: α-pinene is used as a surrogate for all monoterpenes. Isoprene emission is calculated using the parameterised canopy environment emission activity (PCEEA) approach of the MEGAN model. Leaf age and soil moisture are not taken into account in this implementation. Leaf area index (LAI) is prescribed, varying monthly. Emissions of monoterpenes then depend on temperature and LAI only and those of isoprene on temperature, LAI and photosynthetically active radiation. Note that in the formulations provided by these parameterisations, "temperature" means leaf temperature. This is not available in ECHAM5/HAM; instead the lowest model level temperature is used.

Emission of anthropogenic species is according to the EDGAR (fast-track 2000 issue, hereafter FT2000, Olivier et al., 2005). The FT2000 issue does not provide explicit speciation of the emitted volatile organic compounds (VOC), in contrast to the 1990 issue. We assume that the species mix is identical in both. For each gridpoint, the fraction of total VOC that each included species makes up is calculated from the 1990 dataset and applied in turn to the FT2000 dataset to obtain the year 2000 estimate. We model SOA production from toluene, xylene and benzene. The 1990 dataset also includes emissions of trimethylbenzene and a group labeled "other aromatics". Trimethylbenzene is a known SOA precursor (Baltensperger et al., 2005) and is lumped together with xylene. 50 % of the "other aromatics" are also included in this class. No information is available on the diurnal or seasonal variation of anthropogenic VOC emission on a global basis, so emissions are treated as constant in time.

2.2 Formation of SOA

In this model version, due to the heavy computational cost of the many tracers introduced into the aerosol scheme, chemistry is kept to a bare minimum. Oxidation reactions with OH, O_3 and NO_3 are taken into account, but only the major pathways (OH in the case of isoprene and anthropogenics and O_3 in the case of monoterpenes) are considered to produce SOA.

A drawback of this approach is that the known dependency of SOA yield on ambient NO_x (Presto et al., 2005; Kroll et al., 2006; Ng et al., 2007b) is lacking in the model. The entire atmosphere is treated as low-NO_x, a point to which we shall return in the discussion of the model results.

The two-product model of SOA formation is used. This model is founded on the work of Odum and colleagues (Odum et al., 1996), who showed that for a reaction yielding many semi-volatile species, the aerosol yield Y, defined as

$$Y = \frac{\Delta M}{\Delta \mathrm{HC}} \tag{1}$$

where ΔM is the change in aerosol mass and ΔHC is the mass of precursor hydrocarbon consumed, can be modelled by assuming that the reaction produces only two condensable species. In this approach, the gas-phase reaction of a precursor PRE and oxidant OX resulting in the two hypothetical products P_1 and P_2 is described by

$$\mathrm{PRE} + \mathrm{OX} \rightarrow \alpha_1 P_1 + \alpha_2 P_2 \tag{2}$$

where α_1 and α_2 are mass-based stoichiometric coefficients, and subsequent gas-aerosol partitioning by

$$A_i = K_{p,i} M_0 G_i \tag{3}$$

where A_i $(i = 1, 2)$ denotes the mass of product P_i that resides in the aerosol phase and G_i in the gas phase, $K_{p,i}$ is a partitioning coefficient for the organic mass, and M_0 is the total SOA-absorbing mass in the aerosol phase. SOA production is then fully characterised by the four empirical parameters α_1, α_2, $K_{p,1}$ and $K_{p,2}$.

Ng et al. (2007a) found that in the case of low NO_x, SOA formed from xylene, toluene and benzene is effectively non-volatile. This allows us to represent the SOA yield from these precursors in terms of a single product species that, after formation, condenses immediately to the aerosol phase.

The chosen two-product parameters and reaction rates for this model are given in Table 1.

Oxidant concentrations are prescribed as in Stier et al. (2005), except that NO_3 is added using the multi-model mean computed for year 2000 by the RETRO re-analysis project (http://retro.enes.org/index.shtml). The constancy of the oxidant fields over each model timestep makes the system simple enough to solve analytically.

2.3 SOA gas-aerosol partitioning

Equation (3) describes only the partitioning between the gas phase mass and the total aerosol phase SOA mass. In our model, this is not sufficient since we must determine the mass that partitions to each of the size-resolved modes. The underlying theory developed by Pankow (Pankow, 1994a, b) is based on absorption and not adsorption. This means that SOA must be able to partition into the bulk of the material considered as absorber, not just attach to surface sites. For this reason, we exclude black carbon, mineral dust and crystalline salts as SOA absorbers. In the light of the effect of seed particle acidity on SOA discussed by Iinuma et al. (2004), and findings of organosulphates in aerosol (Surratt et al., 2007), this suggests that sulphate may play a role in determining the gas-aerosol partitioning of SOA; however, all such identified mechanisms are chemical and not purely thermodynamic mechanisms, which means that they cannot be quantified through the Pankow theoretical framework. Accordingly, sulphate is not included in M_0 in this model. Regarding aerosol water, we assume that SOA takes up water

Table 1. SOA reaction rates and two-product parameters. MT: monoterpenes, IS: isoprene, TOL: toluene, XYL: xylene, BENZ: benzene. α_1, α_2, $K_{p,1}$, $K_{p,2}$: SOA 2-product parameters (see Sect. 2.2).

Gas	Oxidant	α_1	α_2	$K_{\mathrm{p},1}$	$K_{\mathrm{p},2}$	Source	Rate[4]	Source
MT	O_3	Note 1	Note 2	2.3	0.028	Saathoff et al. (2008)	$6.3\times10^{-16}\exp(-580/T)$	IUPAC
MT	OH	–	–	–	–	–	$1.2\times10^{-11}\exp(440/T)$	IUPAC
MT	NO_3	–	–	–	–	–	$1.2\times10^{-12}\exp(490/T)$	IUPAC
IS	O_3	–	–	–	–	–	$1.03\times10^{-14}\exp(-1995/T)$	IUPAC
IS	OH	0.232	0.0288	0.00862	1.62	Henze and Seinfeld (2006)	$2.7\times10^{-11}\exp(390/T)$	IUPAC
IS	NO_3	–	–	–	–	–	$3.15\times10^{-12}\exp(-450/T)$	IUPAC
TOL	OH	0.36	0	Note 3	Note 3	Ng et al. (2007a)	$1.81\times10^{-12}\exp(338/T)$	MCM[5]
XYL	OH	0.30	0	Note 3	Note 3	Ng et al. (2007a)	2.31×10^{-11}	MCM[5]
XYL	NO_3	–	–	–	–	–	2.6×10^{-16}	MCM[5]
BENZ	OH	0.37	0	Note 3	Note 3	Ng et al. (2007a)	$2.33\times10^{-12}\exp(-193/T)$	MCM[5]

Note 1: Temperature dependent, given as $0.715–0.002T$ by Saathoff et al. (2008).
Note 2: Temperature dependent, given as $1200\exp(-T/35)$ by Saathoff et al. (2008).
Note 3: Treated as non-volatile.
Note 4: T is temperature in Kelvin.
Note 5: Master Chemical Mechanism, University of Leeds, UK, http://mcm.leeds.ac.uk/MCM/.

but water does not absorb SOA. This leaves organic carbon as the only absorber of SOA in the model. We assume uptake of all SOA species by all SOA species and by primary organics.

Consequently, SOA occurs only in modes where POA is present, namely the Aitken soluble and insoluble modes, and the accumulation and coarse soluble modes. In this model version, the nucleation mode contains only sulphate and water. The accumulation and coarse insoluble modes are pure mineral dust modes.

It is shown in the Appendix that the assumption of an activity coefficient of unity for all SOA species is consistent with an equilibrium SOA partitioning between different size classes according to the fraction of non-volatile absorbing aerosol mass in each mode. That is, if M_{NV} and A_i are the total non-volatile absorbing mass and the total aerosol phase mass of the i-th SOA species, and $M_{\mathrm{NV}\,j}$ and A_{ij} the respective quantities in mode j, then

$$\frac{A_{ij}}{A_i} = \frac{M_{\mathrm{NV}\,j}}{M_{\mathrm{NV}}} \tag{4}$$

Hence in the model SOA partitions strongly in favour of the larger modes. Equation (4) has particular consequences for the impact of SOA on cloud condensation nuclei (CCN): since these are larger particles, SOA preferentially condenses on particles that are already of CCN size.

2.4 Measuring model SOA production and lifetime

For semi-volatile species, it is not obvious how to measure the quantity SOA production, since the aerosol mass changes in response to ambient conditions. We can, nonetheless, estimate this quantity for semi-volatile species in another way. While the total net condensation flux is not directly available from the equilibrium partitioning scheme, we do know the total sink flux. On the assumption of source-sink aerosol mass balance over a model integration period, (in which one may have some confidence, if not proof, if the total semi-volatile budget is balanced for the species in question), then the production term may be assumed to be the same as the sum of the sink terms.

The model lifetime τ_M of semi-volatile species in the aerosol phase can be defined as the ratio of the mean aerosol burden $B(t)$ to the integrated production (sink) flux:

$$\tau_{\mathrm{M}} = \frac{\frac{1}{T_2-T_1}\int_{T_1}^{T_2} B\,(t)\,dt}{\int_{T_1}^{T_2} F^{\downarrow}(t)\,dt} \tag{5}$$

where $F^{\downarrow}(t)$ is the sum of the spatially-integrated sink terms, and the model integration runs from time T_1 to T_2. Clearly, τ_{M} is applicable only as a global total metric.

2.5 Aerosol water uptake

The original ECHAM5/HAM water uptake scheme is that of Jacobson et al. (1996), which models water uptake by electrolytic species. In order to take into account uptake of water by organics, the semi-empirical scheme of Petters and Kreidenweis (2007) has been chosen on the basis of its computational efficiency (it requires computation of only a single free parameter κ). For sulphate, sea salt and organic species, the appropriate mean growth factor derived κ value found in Petters and Kreidenweis (2007) is used.

The overall internally mixed aerosol κ is the volume-weighted sum (over the soluble fraction, i.e. in the soluble modes only, and excluding any black carbon and dust) of the individual compound κ values, as per Eq. (7) in Petters and

Kreidenweis (2007). The growth factor can then be calculated using equation (11) in that paper, viz.

$$\mathrm{RH}\exp\left[-\frac{A}{D_{\mathrm{d}}g}\right]=\frac{g^3-1}{g^3-(1-\kappa)} \quad (6)$$

where g is the growth factor, RH the relative humidity (in the cloud-free fraction of the gridbox) on the fractional scale, D_{d} is the particle dry diameter and A is the Kelvin term

$$A=\frac{4\sigma_{s/a}M_{\mathrm{w}}}{\mathrm{RT}\rho_{\mathrm{w}}} \quad (7)$$

where $\sigma_{s/a}$ is the surface tension of water ($0.072\,\mathrm{Jm}^{-2}$) (note that any surface tension effect of the solutes are encapsulated in the κ parameter), M_{w} is the molecular weight of water and ρ_{w} its density. In this implementation, to minimise computational costs, Eq. (6) is solved offline for g as a function of T, RH, D_{d} and κ and the results stored in a lookup table. Once D_{d} and κ have been calculated for each mode, we can then simply look up the growth factor (interpolation to the lookup table values is linear in T, RH and κ, and linear in the logarithm of D_{d}).

2.6 Sink processes for SOA

SOA is subject to wet deposition, dry deposition and sedimentation as for all other model aerosol species. The wet deposition scheme (Stier et al., 2005) calculates partitioning between air and cloud water based on Henry's Law for gases, and based upon prescribed scavenging ratios for aerosols. Separate scavenging ratios are applied per aerosol mode and per cloud type (water, ice or mixed stratiform clouds; convective clouds are always considered mixed). Wet deposition from the cloud is calculated based on the precipitation formation rate. Below cloud, removal of aerosols is calculated as a function of the precipitation flux, the fraction of the gridbox affected by precipitation, and prescribed (again, per mode) collection efficiencies for rain and snow. Below-cloud scavenging of gases is not included. The scheme also allows for re-evaporation of rain beneath precipitating clouds.

The dry deposition scheme calculates dry deposition velocities v_{d} using a serial resistance approach. For gases, v_{d} is calculated from the aerodynamic, quasi-laminar boundary layer, and surface resistances according to the "big leaf" concept (Ganzefeld and Lelieveld, 1995; Ganzeveld et al., 1998) for each of the model fractional surface cover types (snow/ice, bare soil, vegetation, wet skin, water and sea ice) of each surface grid box. Surface resistances are prescribed for SOA species. For aerosols, v_{d} is a function of particle size, density, turbulence and surface cover type.

2.7 SOA and cloud processes

In the simulations described herein, cloud droplet activation is calculated according to the scheme of Lin and Leaitch (1997), in which only the aerosol size, not its composition, is taken into account. Thus in the model, SOA affects cloud droplet number only through its effect on particle size, not through hygroscopicity, nor by affecting the surface tension of droplets. The coupling of aerosols to the large-scale cloud microphysics scheme allows the aerosol to affect cloud lifetime as well as droplet number.

Clouds affect SOA through the above-described wet sink processes.

No aqueous-phase SOA chemistry is included. This omission will bias the model both towards too low SOA mass and too much high-volatility SOA. This is because aqueous phase reactions both produce SOA (for example, organic acids such as oxalic and malonic acids) and because aqueous phase reactions produce SOA that is of lower volatility than the analogous gas-phase reactions (Hallquist et al., 2009 and the references therein).

3 Model results

The simulations described herein are simulations of the year 2000. The model dynamics (vorticity and divergence of the wind field, temperature and surface pressure) are calculated in spectral space with triangular truncation at term 63 (T63), while physics are calculated on a $1.8^\circ \times 1.8^\circ$ Gaussian grid (Roeckner et al., 2003). The simulations use 31 vertical levels, from the surface to 10 hPa. The model diagnostics are output every 6 simulated hours. Large-scale meteorology is constrained by nudging towards the ECMWF analysis for the year 2000.

Three simulations were performed: one without SOA, one with SOA and one with only biogenic SOA. The results of the latter are very similar to those of the simulation with all SOA, and in the following we will describe the results in terms of the simulations without SOA and with all SOA. Where results of the simulation with biogenic SOA only are presented, this is specifically mentioned. The simulation with SOA is referred to as "SOA" in the figures, and the simulation without SOA as "no SOA".

3.1 SOA precursor emissions

The annual emission flux of each anthropogenic precursor is shown in Fig. 1.

Toluene and xylene emissions are closely connected to fossil fuel production and use, and emission of these species is greatest in north-western Europe, the north-eastern United States and in East Asia. Benzene is a known carcinogen and is tightly regulated in the United States and Europe; it has greatest emission in South and East Asia.

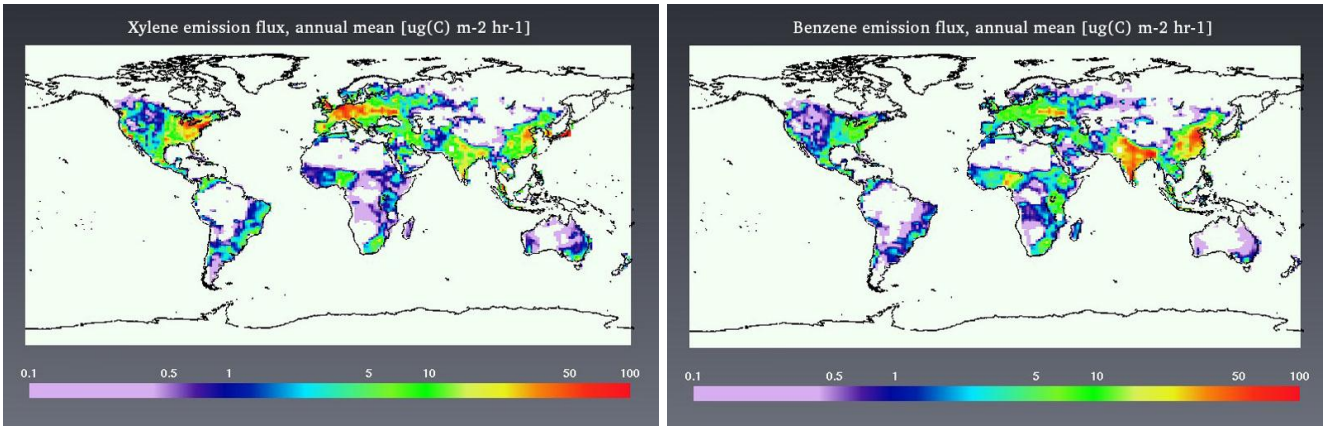

Fig. 1. Anthropogenic SOA precursor emissions.

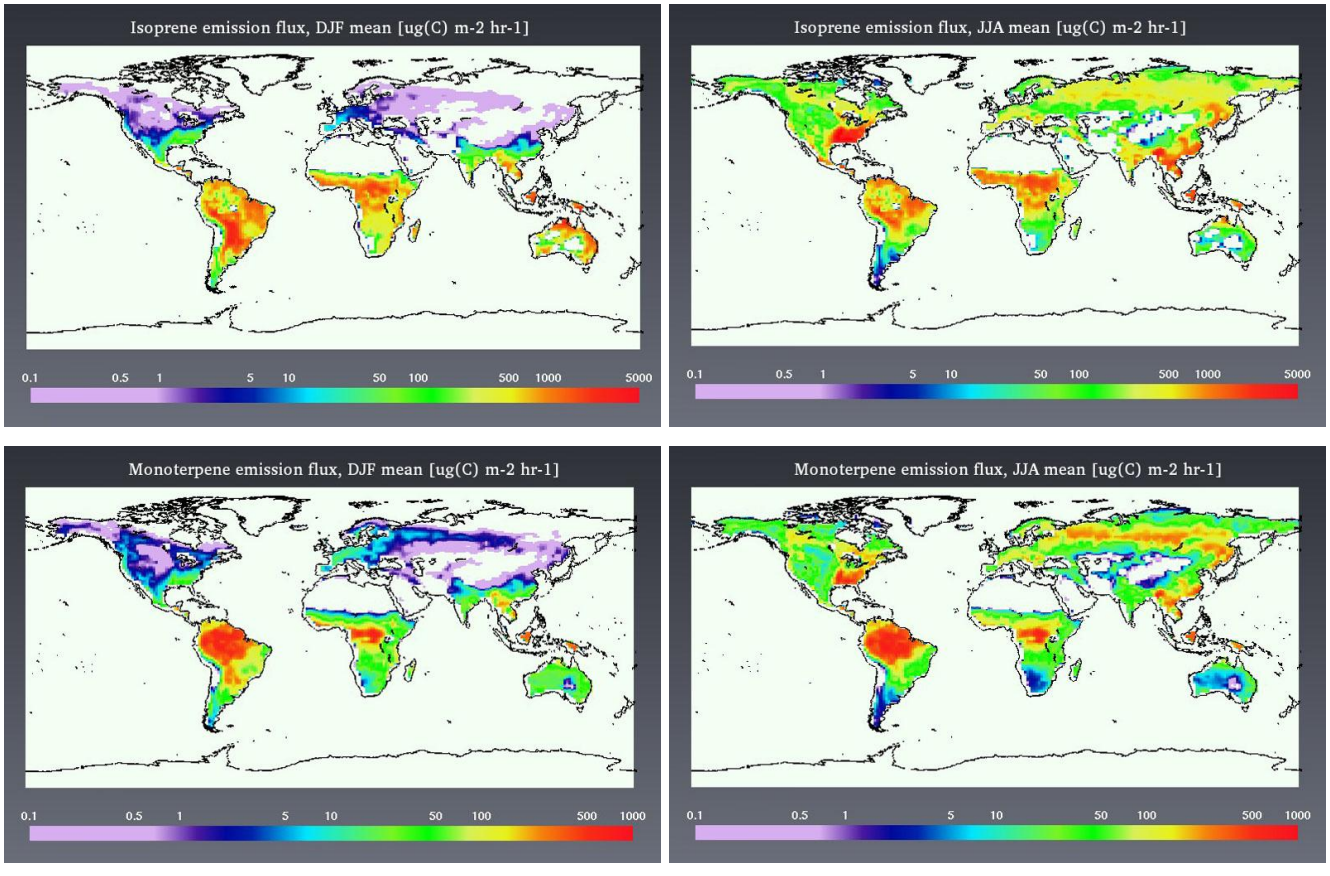

Fig. 2. Seasonal variations of biogenic emissions.

Mean wintertime and summertime emissions of isoprene and monoterpene emission are shown in Fig. 2. Observe that different scales are used for isoprene and for monoterpenes. Global annual totals are calculated as 446 Tg yr^{-1} isoprene and 89 Tg yr^{-1} monoterpenes. These figures are somewhat lower than those of Guenther et al., 2006 (600 Tg yr^{-1} isoprene) and Guenther et al., 1995 (127 Tg(C) yr^{-1} monoterpenes), but within the uncertainty ranges of those estimates. This compares with a figure of 17 Tg yr^{-1} for the sum of the anthropogenic precursors (6 Tg yr^{-1} toluene, 6 Tg yr^{-1} xylene and 5 Tg yr^{-1} benzene).

Biogenic emissions are predominantly tropical, with more than 75 % (on an annualised basis) of biogenics originating from these latitudes. Boreal forest emissions are significant in the summer months, but weak in wintertime.

Table 2. Budget of modelled SOA per precursor species. (a): aerosol, (g) gas phase species. Dep.: deposition, Sed: sedimentation.

SOA Precursor	Prod[1] [Tg yr^{-1}]	Wet Dep.(g) [Tg yr^{-1}]	Wet Dep.(a) [Tg yr^{-1}]	Dry Dep.(g) [Tg yr^{-1}]	Dry Dep.(a) [Tg yr^{-1}]	Sed [Tg yr^{-1}]	Balance[2] [%]	Burden [Tg]	Lifetime [days]
Isoprene	17	64	16	24	0.70	0.027	3.0	0.71	15.5
Monoterpenes	4.0	6.0	3.7	2.8	0.32	0.013	2.0	0.064	5.8
Anthropogenics	5.6	0	5.3	0	0.26	0.032	0.75	0.074	4.8

[1] production of SOA from isoprene and monoterpenes is estimated as Wet Dep(a) + Dry Dep(a) + Sed.
[2] (production-all sinks)/production, absolute value.

3.2 SOA budget

The model SOA mass budget is presented in Table 2.

Anthropogenic precursor emissions having no diurnal or seasonal variation in the model, the seasonal variability in anthropogenic SOA production is rather limited, with monthly global total production varying from 0.42 to 0.50 Tg month^{-1}. The global maximum production takes place in Northern Hemisphere (NH) spring. This is due to a precursor reservoir that is built up at high latitudes during the winter, when the photochemical sink is weak. Europe, the United States, Japan, China and India are the main source regions for anthropogenic SOA.

Production of biogenic SOA species, since these are semi-volatile, is only possible to estimate as a global total according to the methodology of chapter 2.4. This gives estimates of 17 Tg yr^{-1} and 4.0 Tg yr^{-1} aerosol from isoprene and monoterpenes respectively. Together with the estimated 5.6 Tg yr^{-1} from anthropogenic precursors, this gives total SOA production of approximately 27 Tg yr^{-1}, compared with the total model POA sources of 47 Tg yr^{-1}.

For the non-volatile species, the sink fluxes are in much the same ratios as for primary OC, with wet deposition removing over 90 % of the aerosol mass from the atmosphere. One may note that despite the affinity of SOA for larger aerosol particles in the model, sedimentation remains a very weak sink for organic mass. This is especially so for the biogenic species, most likely because they are semi-volatile and evaporate in warm near-surface conditions.

For semi-volatile SOA formed from isoprene and monoterpenes, the largest sinks are directly from the gas phase.

The modelled seasonal mean anthropogenic and biogenic SOA burdens are shown in Figs. 3 and 4 respectively.

It is notable that the model isoprene-derived SOA burden exceeds that of SOA from all other sources, and that its estimated lifetime is also much larger. This is due to the particular vertical distribution of model isoprene SOA, which is discussed in chapter 3.4.

3.3 Geographical and seasonal distribution of SOA

A combination of high emissions and active photochemistry gives a high anthropogenic SOA burden over south and southeast Asia, weakening in the summer with the enhancement of the wet deposition sink. Low wintertime OH levels north of 45° N lead to very little SOA formation despite substantial precursor emissions from Europe and the northeastern United States.

The biogenic SOA loading is strongly dominated by the contribution of tropical forests, with a comparatively small (on an annualised basis) input from the Boreal forest. In particular, the peak in September-November in the Amazon is related to the biomass burning season. SOA formation is related to the amount of organic absorbing material (M_0) in the ambient aerosol. The high organic loading in the biomass burning season therefore leads to enhanced SOA formation. In reality, this effect will be mitigated by the soil dryness (which reduces plant emissions) and the destruction of biomass, effects that are not accounted for in the model. Elsewhere, the "biogenic hotspot" in the southeastern United States is clearly visible in the summer months. Also worth remarking upon is the relatively low burden over the forests of Indonesia and Papua New Guinea, despite the high precursor emissions in those areas. Heavy model precipitation in that region efficiently removes SOA through wet deposition.

3.4 Vertical distribution of SOA

Vertical transport plays a crucial role in model SOA formation. Convection lifts gas-phase condensable species to much colder regions of the atmosphere, where partitioning favours the aerosol phase. The common occurrence of deep convection in the tropics thus enhances SOA formation, already favoured due to high precursor emissions and strong photochemistry. Kulmala et al. (2006) suggested a similar mechanism for insoluble organics.

The simulation without SOA, with values of less than 5 ng m^{-3} above 8 km, cannot explain observations of organic aerosols (Murphy et al., 1998; Froyd et al., 2009; Morgan et al., 2009) in the upper troposphere. The annual zonal mean of total organic aerosol mass is presented in Fig. 5.

The two-product model of SOA formation is clearly visible in the modelled vertical profile of biogenic SOA (Fig. 6). For each modelled biogenic precursor, we have two SOA products of differing volatilities. The more volatile products

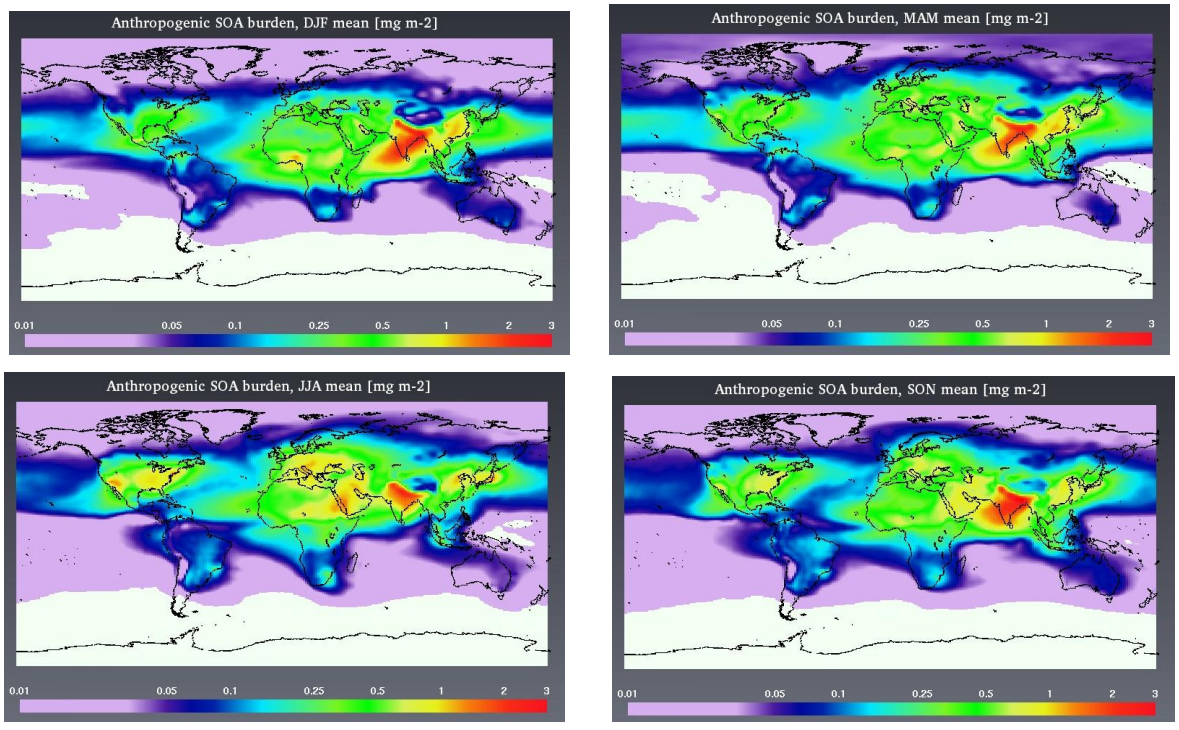

Fig. 3. Seasonal mean anthropogenic SOA burdens.

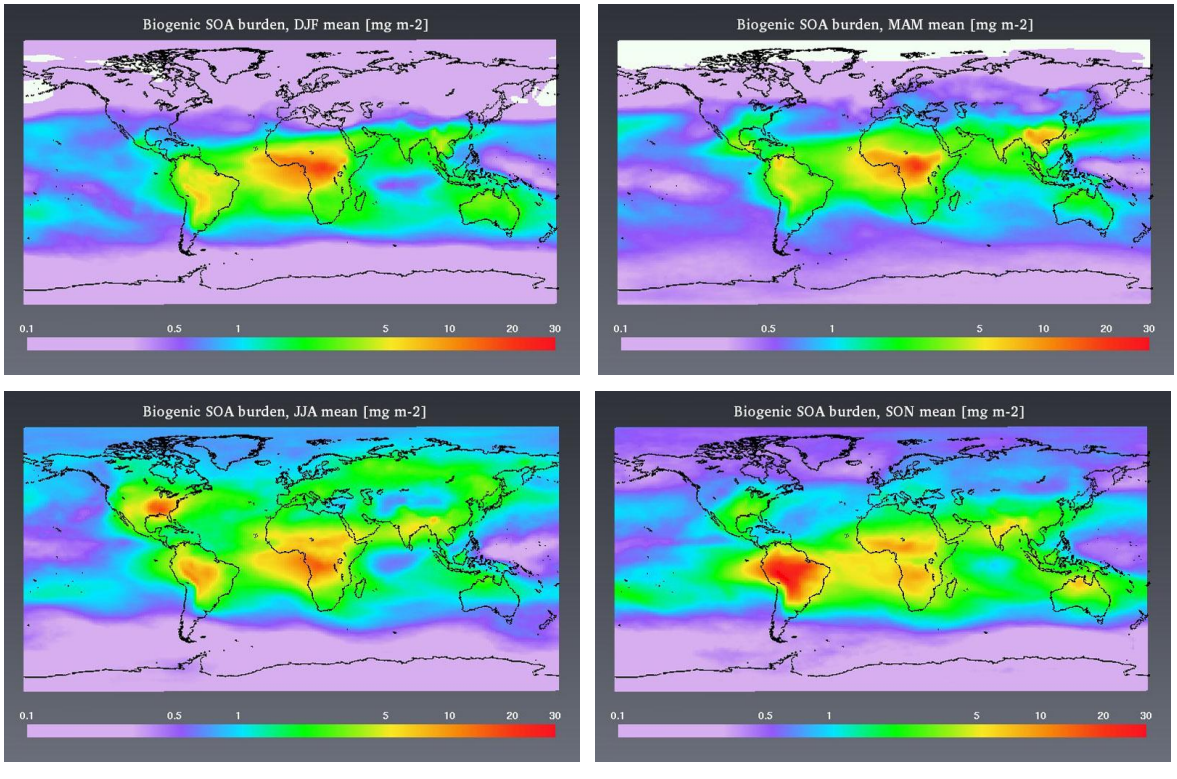

Fig. 4. Seasonal mean biogenic SOA burdens.

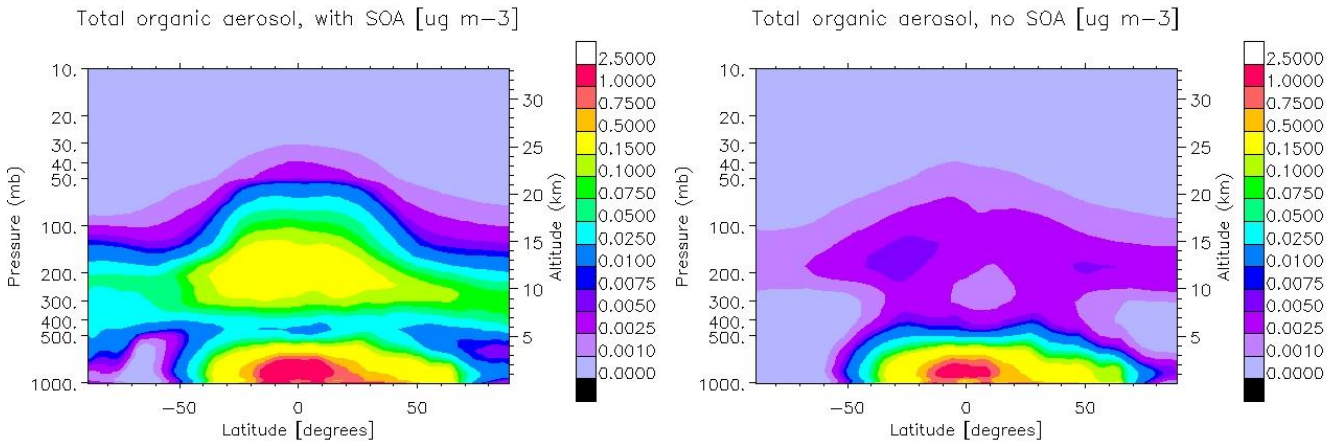

Fig. 5. Annual zonal mean total particulate organic matter (POM) with SOA (left) and without SOA (right).

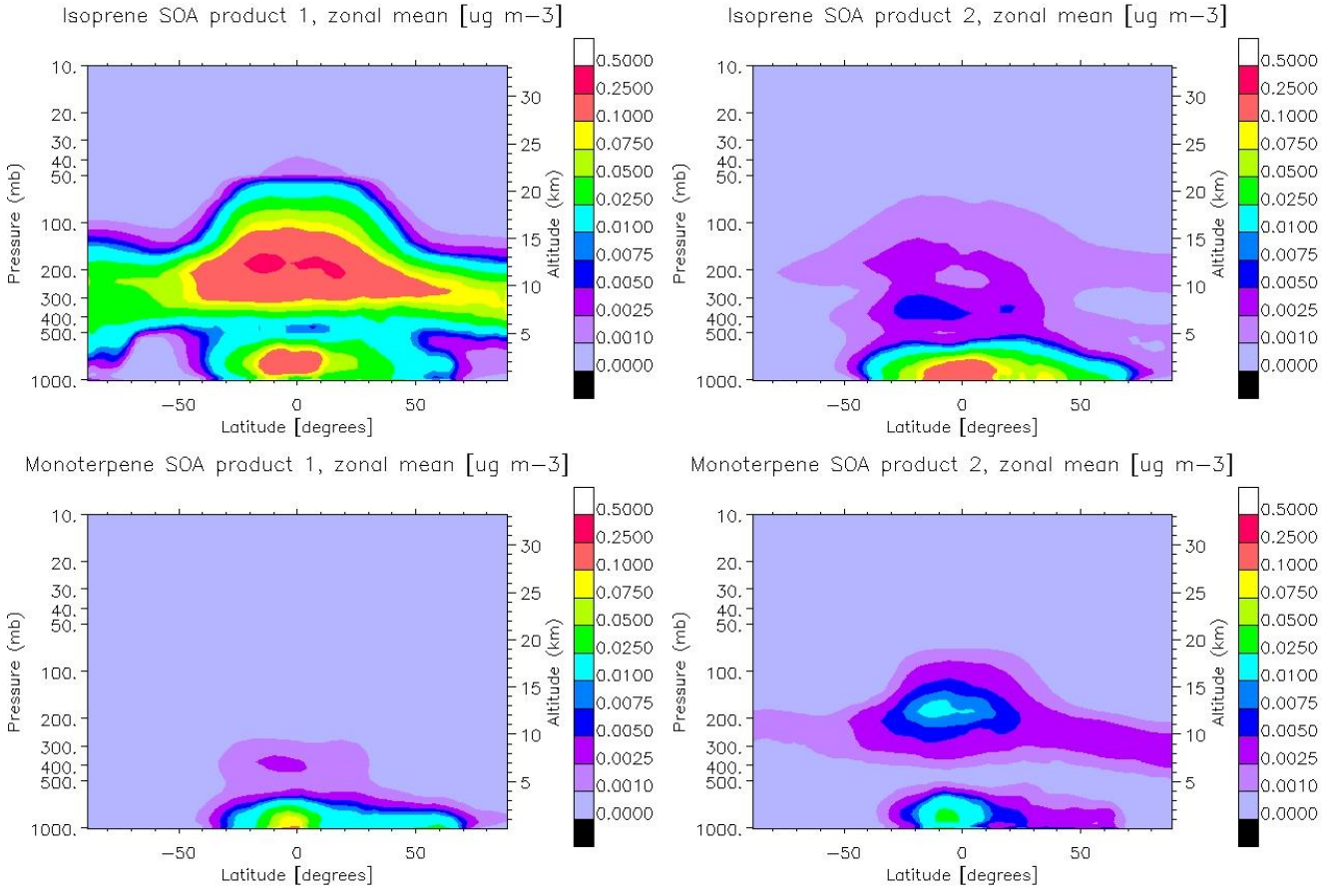

Fig. 6. Vertical profile of aerosol phase mass of each model semi-volatile species.

require lower temperatures for the gas-aerosol partitioning to favour the aerosol phase. The split is clearly visible in the vertical profile. In reality, SOA is composed of a range of compounds of differing volatilities, so that the two peaks of the model distribution is unlikely to be an accurate reflection of true vertical distribution.

A high-altitude SOA pool is formed mainly in the tropical mid- to upper troposphere at altitudes of approximately 8–16 km, and at temperatures of less than 240 K, mainly from isoprene product 1 (the high-volatility product). This pool is subsequently transported worldwide.

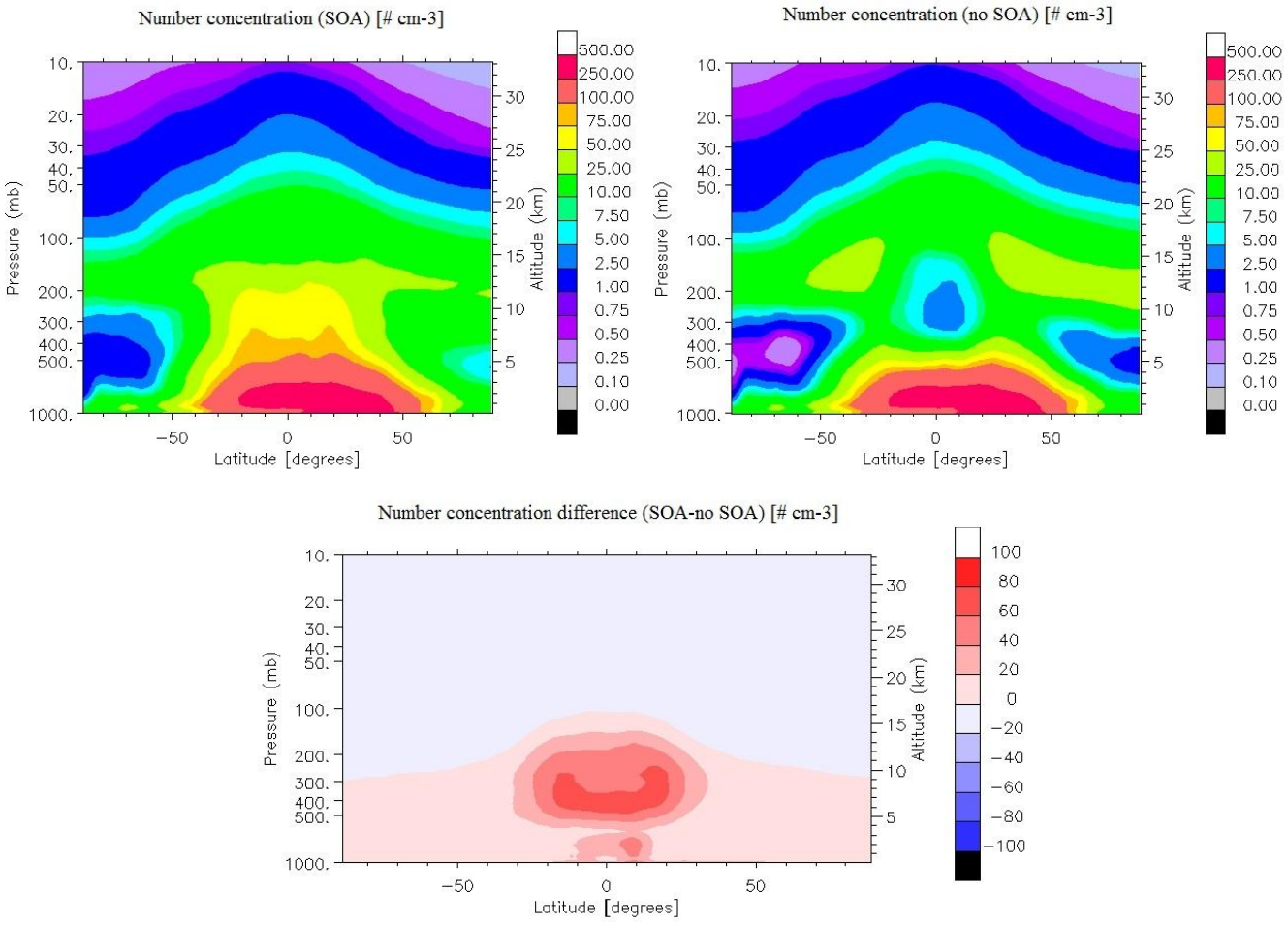

Fig. 7. Accumulation soluble mode number concentration (# cm^{-3}) with SOA (above left), without SOA (above right) and the difference (below).

The high upper-tropospheric loading of isoprene-derived SOA requires close examination. It comes about as a result of the two-product properties of isoprene-derived SOA, in particular those of product 1, for which the laboratory data chosen (Henze and Seinfeld, 2006) gives a stoichiometric yield of 0.232 and a partitioning coefficient of 0.00862 m^3 µg at 295 K. The former implies an input to the atmosphere (assuming OH supply is non-limiting) of some 100 Tg yr^{-1} condensable gas from the model isoprene emissions of 446 Tg yr^{-1}. The latter implies that the compound so formed is highly volatile and favours the gas phase down to very low temperatures. The combination of high yield and high volatility results in an aerosol species that condenses primarily in the upper troposphere, at temperatures too cold for liquid water. The high altitude and lack of wet removal (SOA in the model does not interact with ice) lead to the high modelled burden and extended lifetime.

3.5 Impact of SOA on aerosol number concentration

Since SOA condenses onto pre-existing aerosol, one would intuitively expect that the main effect of SOA on aerosol number is to boost some of the population of the smaller modes into the larger size ranges. This is indeed so in the zonal and annual mean: in particular, the soluble accumulation mode number concentration is increased at the expense of the soluble Aitken mode. The zonal mean number concentrations of these modes are shown in Figs. 7 and 8 respectively. Numbers are also enhanced in the coarse mode, though the effect is rather small compared to the accumulation mode.

The increase in the number of larger particles enhances the coagulation sink of small particles.

Number concentrations in the nucleation and Aitken modes are depleted in the simulation with SOA compared to that without SOA. For the nucleation mode (which in the model contains only sulphate and water, not SOA) the effect is minor. Aitken insoluble particles are associated with

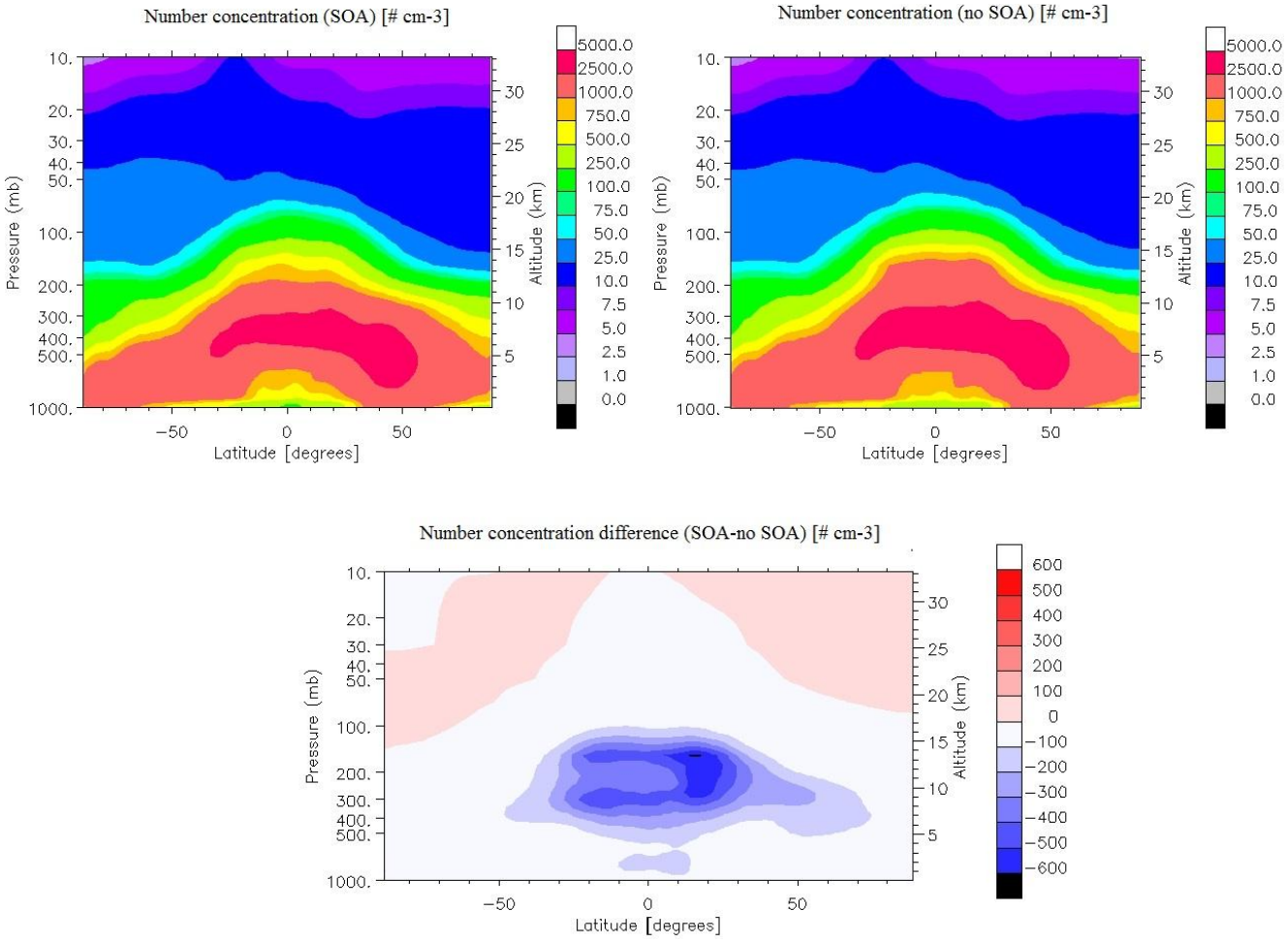

Fig. 8. Aitken soluble mode number concentration (# cm^{-3}) with SOA (above left), without SOA (above right) and difference (below).

anthropogenic emissions in the model, and converted to soluble by condensation of sulphuric acid and by coagulation with the soluble modes, and hence generally confined to the lower and mid-troposphere. The influence of SOA on this mode is also minor.

3.6 Aerosol optical properties

The model global annual mean aerosol optical depth at 550 nm is 0.13, compared to 0.12 without SOA. The annual mean AOD is shown in Fig. 9. Seasonal and regional variations in the AOD difference follow the variations of the SOA burden, as discussed in chapter 3.5, reaching a local maximum of about 0.2 in the Amazonian basin in the biomass burning season.

3.7 Direct and indirect effects of SOA

Finally, we present the modelled influence of SOA upon climate in terms of radiative effects. We do not attempt to estimate the radiative forcing in terms of present minus preindustrial climate, since the biogenic emissions model requires a gridded dataset of emission factors, that depend on the vegetation present in the grid cell, and which is available only for present-day conditions. An estimate of the radiative forcing due to SOA requires that changes in land cover, especially tropical deforestation, are taken into account, which is beyond the present capabilities of this model. Instead, we estimate the direct effect as the difference in the top of the atmosphere (ToA) net radiative flux under clear-sky conditions between a simulation including SOA and a simulation with zero SOA, with the large-scale meteorology constrained by nudging as described in the introduction to chapter 3. The indirect effect is the difference in the TOA fluxes under cloudy (all-sky minus clear-sky) conditions.

The direct effect is shown in Fig. 10. On the global annual mean, it amounts to a cooling of $-0.31\,Wm^{-2}$, with peak cooling of approximately $-2\,Wm^{-2}$ in the southwest of the Amazon basin, where the Andes form a barrier (compare the maximum annual burden in Fig. 4). Some small positive values can be seen, mainly over Greenland and Antarctica.

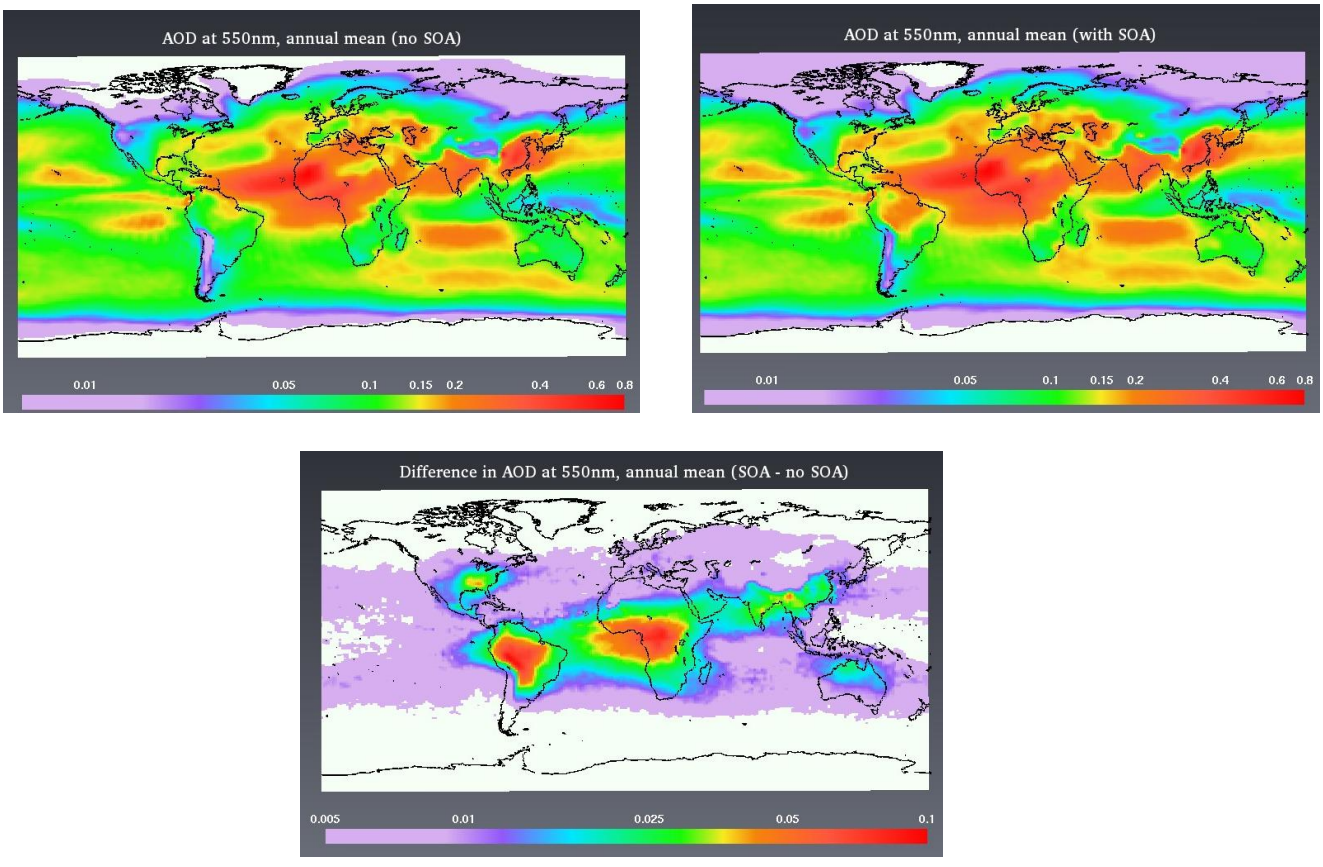

Fig. 9. AOD at 550 nm with SOA (above, left), without SOA (above, right) and the difference (below).

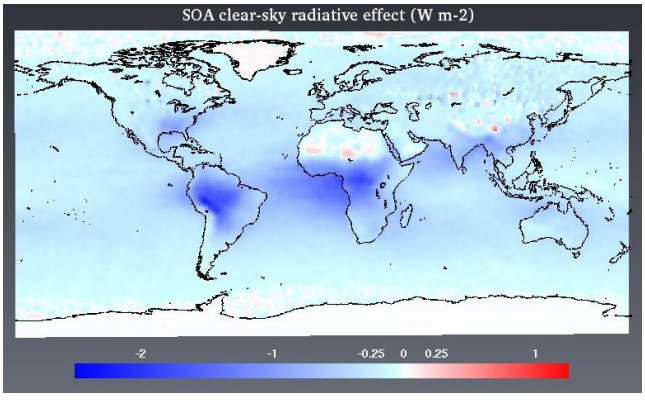

Fig. 10. Difference in clear-sky top of atmosphere SW flux (SOA – no SOA).

These are connected with the changes in the particle diameter towards the larger size range, which is most pronounced in these regions. Larger particles scatter more radiation in the forward direction, and thus less radiation is lost to space than would be the case with the same number of smaller particles of identical composition. Elsewhere, it is noteworthy that the boreal forest contributes significantly only in the northern hemisphere summer (not shown) and little in the annual mean.

The biogenic SOA only simulation gives a clear-sky effect of $-0.29\,\mathrm{Wm}^{-2}$.

The modelled summertime and wintertime mean cloud droplet number concentrations (CDNC) at 900 hPa are shown in Fig. 12. The time averaging takes into account only time when cloud is present. Stratiform cloud decks often cover only a single model level. In the NH winter, a reduction in CDNC can be seen over Europe and parts of China; in the NH summer, a smaller reduction can be seen over Japan and off the West African coast.

The model gives a noisy result for the SOA indirect effect (Fig. 11). For this reason, Fig. 11 has been subject to a 9-point smoothing algorithm. The modelled indirect effect of SOA is clearly positive in some regions: north-western Europe, especially the North Sea, Japan and the surrounding maritime area, much of South America and the West African coast from approximately the equator to 20° S.

This is related to seasonal perturbations of stratus decks in anthropogenically influenced (whether by industry or biomass burning) areas. The mechanism appears to be as

follows: in the model, the Lin and Leaitch activation scheme is used, whereby any soluble particle with radius of at least 35 nm can act as a cloud condensation nucleus (CCN), independently of its chemical composition. In this model scheme, SOA partitions preferentially to large particles (thus, to those that are already of CCN size). Therefore, in the model, SOA in the polluted areas leads to an increase in the radius of CCN-sized particles without increasing their number, thus opposing the first indirect effect. In the presence of a sufficient number of larger particles, the condensable SOA supply is essentially exhausted by those particles, leaving very little growth "fuel" for small particles, while at the same time enhancing the coagulation sink for the small particles. The net result is a decrease in CCN. On the other hand, if there are few large particles available, SOA will drive growth of small particles and this can result in an increase in CCN. Globally, the modelled global mean SOA indirect effect is a warming of $+0.23\,\mathrm{Wm}^{-2}$.

Since the indirect effect of SOA is a short-term response generated by the presence of large numbers of anthropogenic particles, it is probably more appropriate to consider it as an anthropogenic forcing, rather than a natural feedback in the climate system. However, for the purposes of calculating an overall effect of SOA, it will be treated as a feedback.

Longwave (thermal) radiative effects, are a global clear-sky total of $+0.02\,\mathrm{Wm}^{-2}$, and an indirect effect of $-0.03\,\mathrm{Wm}^{-2}$.

Assuming additivity of these effects, the overall model estimate of the climate impact of SOA under year 2000 conditions is therefore $-0.09\,\mathrm{Wm}^{-2}$.

4 Model evaluation

4.1 Comparison with measurements

For evaluation of global aerosol-climate models, measurements of modelled species over wide areas and long time intervals are desirable. Unfortunately, few such data sets are available as far as organic species are concerned, and none that explicitly provides SOA data. Long-term and wide-area measurements are almost invariably clustered in economically advanced countries. In view of the importance of tropical regions to the model, this situation is not optimal. However, lacking better alternatives, in this chapter, we compare measurements of organic carbon (OC) aerosol mass taken in Europe and the United States against model values calculated at the same points.

When one considers semi-volatile species, because of the sensitivity of SOA partitioning to temperature, measurements must necessarily be made at ambient temperatures. In particular, if one is to compare model against measurements in the free or upper troposphere, such measurements must be made in-situ and not, for example, by collection on filters and subsequent ground-level analysis. Unfortunately, such measurements that can explicitly give organic mass (rather than, for example, an organic to sulphate mass ratio, e.g. Froyd et al., 2009) are scarce. Some information about the performance of the updated model in the whole atmospheric column may be obtained from optical measurements. To this end the Aeronet (Holben et al., 1998) network of measurement sites is used.

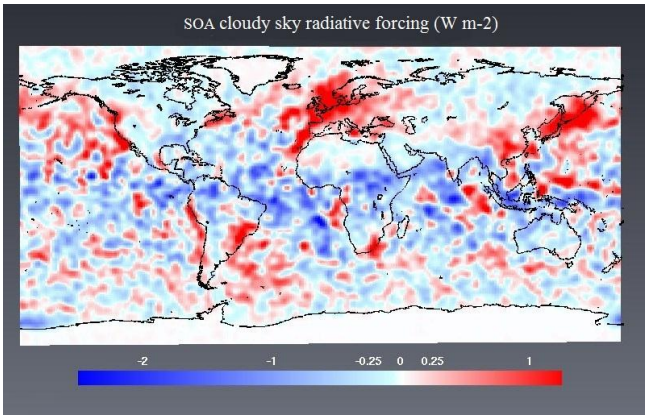

Fig. 11. Annual mean SOA indirect effect.

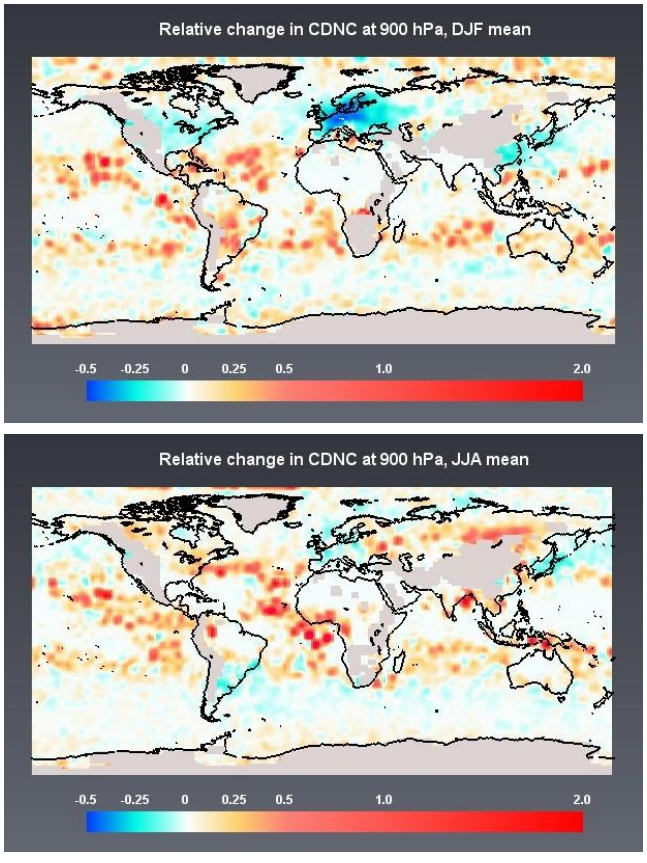

Fig. 12. Change in CDNC (SOA-no SOA) in the DJF mean (above) and JJA mean (below) at 900 hPa. Gray shading indicates land height above that level.

Table 3. Comparison of model results with mean and median observed quantities.

Quantity	Observed	Model, no SOA	Model, with SOA
IMPROVE mean OM mass ($\mu g\,m^{-3}$)	1.84	0.74	1.2
IMPROVE median OM mass ($\mu g\,m^{-3}$)	1.46	0.36	0.64
EMEP mean OM mass ($\mu g\,m^{-3}$)	3.85	0.90	1.4
EMEP median OM mass ($\mu g\,m^{-3}$)	3.49	0.69	1.1
AERONET mean AOD, mid-visible	0.225	0.13	0.15
AERONET median AOD, mid-visible	0.169	0.10	0.12
AERONET mean AOD, near IR	0.117	0.082	0.094
AERONET median AOD, near IR	0.088	0.067	0.077

The biogenic emission model is evaluated in the work of Guenther et al. (2006) and Guenther et al. (1995) and this work is not repeated here.

All measurements are quoted in mass of organic aerosol (not mass of organic carbon).

Monthly mean and median values of the observed organic aerosol mass concentration from EMEP and IMPROVE and of AERONET AOD observations are presented and compared with the model results with and without SOA in Table 3.

4.1.1 North America

The IMPROVE (**I**nteragency **M**onitoring **Pro**tected **V**isual **E**nvironments) network (http://vista.cira.colostate.edu/improve/) has recorded aerosol properties over the contiguous United States since the 1980s, and, as its mission is primarily to monitor visibility at places of outstanding natural beauty, it is a rural network. The network measurement dataset has been analysed for the same period (namely July 2002–June 2003) that covers the European EMEP EC/OC campaign, which is analysed in the following chapter. The IMPROVE observations of OC for this period consists of a total of 1915 monthly mean observations from ca. 60 stations (not all stations reported during each month of this period). For comparison, the model was run for the same time period (after spinup), nudged to ECMWF analysis, with and without SOA. The quoted IMPROVE measurements are for $PM_{2.5}$.

The distributions of observed and modelled OC mass are presented in Fig. 13 as frequency of observed/modelled mass in bins of $0.5\,\mu g\,m^{-3}$. Also shown is the monthly mean of all stations in the network versus the mean of the model calculations for the same sites.

Wildfires are, episodically, a major factor in aerosol loading at some of the IMPROVE stations (observations of organic carbon are as high as $57\,\mu g\,m^{-3}$ in the monthly mean in the study period). Real fire events are not always present in the model, and in such cases very large differences between model and observations occur. Another consequence is that

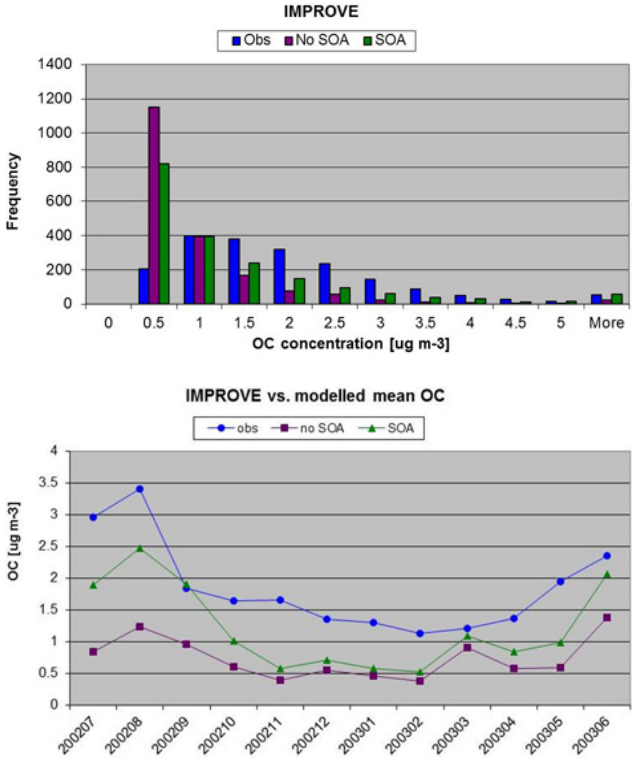

Fig. 13. IMPROVE observations and modelled OC aerosol mass.

the standard deviations of these datasets are very large. These factors destroy any overall correlation between the observations and modelled data. Also, while some improvement in agreement on the large scale between model and observations is visible from Fig. 13, it is notable that the observations remain consistently higher than modelled OC concentrations, particularly in winter time.

The distribution of IMPROVE observations exhibits a single peak near $1\,\mu g\,m^{-3}$. Clearly, the simulation with SOA better approaches the observed distribution: however, the occurrence of low total POM is still much higher in the model than in observations.

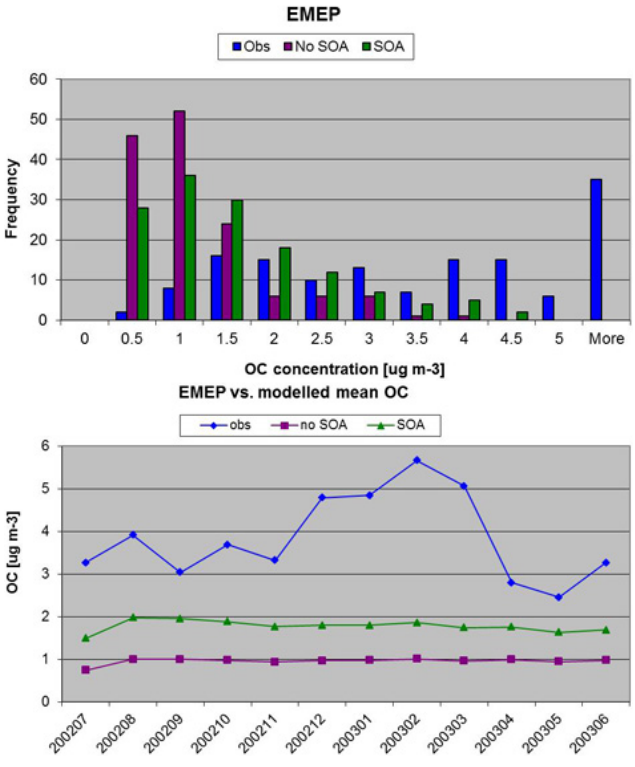

Fig. 14. EMEP observations and modelled OC aerosol mass.

4.1.2 Europe

A one-year-long measurement campaign (called the EC/OC campaign) was carried out by the European Monitoring and Evaulation Programme (EMEP) from July 2002–June 2003. Twelve stations participated in the campaign. One station (Kosetice, Czech Republic) did not report data for the first two months of the campaign, giving a total of 142 monthly mean observations.

The EC/OC campaign results document PM_{10} measurements only. This is potentially important, since the model is not designed to include large particles, as those particles are less radiatively active and have short atmospheric lifetimes (recall that the coarse mode in the model consists of a log-normal distribution of particles larger than 1 µm diameter). A sample containing a significant proportion of OC mass in particles of the uppermost size range of PM_{10} is therefore not possible to capture with the model.

Measurements from the EC/OC campaign are compared against model results in Fig. 14.

While the inclusion of SOA increases the total modelled organic mass substantially (by 50 % on the average of all sites for the year in question), in general the modelled mass remains well short of the measured OC mass. Only at one site (Kollumerwaard, Netherlands) and for three out of twelve months does the modelled mass equal or exceed the measured mass, and this is the case only for the simulation with SOA. This difference between model and observations is particularly large in the more southerly sites in wintertime, when the large organic peaks observed at Ispra, ISAC Belogna (Italy) and Braganca (Portugal), sites that are located at latitudes between 42° N and 46° N, are absent in the model.

The model capture of seasonal variation may be measured by the correlation between model and measurements. For Europe this is, as a whole, poor: only 0.42 for the full measurement dataset (without SOA) and even poorer, 0.39, with SOA. Excluding the three southern European stations at Bracanga, Ispra and ISAC leaves better agreement of the variation of model and observations, with a correlation of 0.70 between observations and model without SOA and 0.75 with SOA. The mean of the observations excluding these stations is 3.1 µg m^{-3}, compared with modelled values of 1.0 µg m^{-3} (without SOA) and 1.4 µg m^{-3} (with SOA). On this basis, the model seems to reflect the seasonal variation in total OC reasonably well in the northern and central Europe, even though the magnitude remains short of the measurements. In the south, however, the model differs by up to an order of magnitude to observed OC values. In addition, it is temporally anti-correlated to observations in that region.

For most stations in the EMEP network, and particularly for the southern stations, total OC and EC are very strongly related. Overall correlation of EC to OC is 0.83; for measurements excluding the three southern sites, 0.65; and for measurements at the three southern sites, 0.95. This can arise beause the OC is largely anthropogenic, or because anthropogenic OC enhances the biogenic OC mass by providing additional SOA absorbing mass (e.g. Carlton et al., 2010), or both.

4.1.3 Aeronet

Aeronet observations over the period of the EMEP EC/OC campaign comprises a total of 845 monthly mean observations at locations spread worldwide (but not uniformly, so that, for example, aeronet means are not comparable to satellite-derived global means). Aeronet observations include aerosol optical depth (AOD) measurements at different wavelengths. The wavelengths measured depend upon the measuring site, but measurements at 500 nm and 875 nm are commonly available. The model diagnostic AOD is calculated at 550 nm and 825 nm, so that although we are not comparing identical quantities, they can be expected to be very closely related. The distribution of measured and modelled mid-visible AOD at the aeronet sites is shown in Fig. 15.

The incidence of very low (less than 0.05) mid-visible AOD in the model is reduced by about 20 % in the simulation with SOA compared to that without SOA, but low AOD remains much more common in the model than in the aeronet observations. Otherwise, the distribution is moved slightly in the direction of higher AOD. Results for the near-infrared AOD are broadly similar, with a reduction in the incidence of modelled low AOD and increase in that of high AOD.

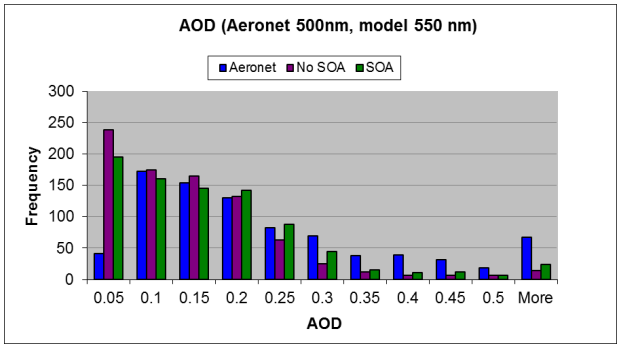

Fig. 15. Distribution of measured and modelled AOD in the mid-visible.

With the inclusion of SOA, the correlation between Aeronet observations and model increases marginally, from 0.71 to 0.73 for the mid-visible AOD, and from 0.66 to 0.67 for the near-infrared AOD.

No systematic difference between the simulations with and without SOA is apparent when comparing against the Aeronet-measured Ångström parameter.

4.2 Comparison with other models

Due to the importance of isoprene to the results, this model inter-comparison is limited to those studies which include isoprene as a SOA precursor. In Table 4, the emissions, production and burdens calculated by previous studies and this study are listed. Emissions of isoprene, monoterpenes and anthropogenics are denoted E_i, E_t and E_a and are given in Tg(C) yr^{-1}. Production and burdens of the respective species are denoted P_i, P_t, P_a, B_i, B_t and B_a, and the total SOA burden by B_{tot}. Production figures are in Tg yr^{-1} and burden figures in Tg unless otherwise stated.

Model biogenic emissions are generally in good agreement, with the exception of the low isoprene emissions of Hoyle et al. (2007) and the low monoterpene emissions of Heald et al. (2008). This must, however, be viewed with caution. MEGAN and its predecessors, especially Guenther et al. (1995), underlie most global biogenic emission models, and therefore a comparison of ostensibly different models is to a large extent comprised of a comparison of different implementations of the same underlying parameterisation. This can give one the illusion that estimates of global biogenic emissions are well-constrained, when this is not the case. This subject is analysed in more detail by Arneth et al. (2008), who point out that global estimates of biogenic emissions remain poorly constrained, despite the seeming agreement among models.

The ostensibly good agreement in total SOA burden between the models belies the wide differences in SOA production and in burdens of individual species, and any such agreement must therefore be regarded as coincidental. Production figures must be viewed with caution, since, as discussed in chapter 2.4, the definition of "SOA production" is not clear when applied to semi-volatile species, and none of the studies listed specifies how exactly the model in question calculates this diagnostic. There are substantial differences between the model choices of SOA production pathways. For example, Hoyle et al. (2007), following Chung and Seinfeld (2002), assume unity mass yield of SOA from all monoterpenes under NO_3 oxidation (using β-pinene as surrogate species), whereas the study of Tsigaridis and Kanakidou (2007) and this study assume zero SOA yield for this case (using α-pinene as surrogate species). Both these approaches are valid, based on the selection of the surrogate species (Hoffman et al., 1997).

Other key differences include the nature of the models: all models in the listed studies except this study include full chemistry models with prognostic OH, O_3 and NO_3, compared to the highly simplified scheme and prescribed oxidant values in this model. This study is the only one of those listed that uses a size-resolved aerosol model with detailed microphysics and coupling to cloud processes. TM3, GEOS-CHEM and OSLO CTM2 are all offline chemistry-transport models (CTMs) that are driven by prescribed meteorological datasets. Tsigaridis et al. (2007) simulated the year 1990, whereas Hoyle et al. (2007) and Henze et al. (2008) simulated the year 2004, but using different meteorological datasets. The two online models, Heald et al. (2008) and this study, both simulated the year 2000. The consequent meteorological differences between the models can lead to variations in emissions (of biogenic precursors), in SOA formation, in convective and advective transport, and in sink processes.

The models also differ in resolution in both the horizontal and the vertical. This gives rise to differences in numerical diffusion between models, which causes further variation in the transport of aerosols and gases.

5 Discussion

5.1 SOA production

5.1.1 SOA precursors

There are known SOA precursors, both biogenic and anthropogenic, that are not included in the model. These include methyl chavicol and sesquiterpenes (Lee et al., 2006), emissions of which remain unquantified. The latter class of compounds may be important in new particle nucleation: this is further discussed by Bonn et al. (2003) and Bonn et al. (2008). Furthermore, they have high molecular weight, and are known to have a high aerosol mass yield (Lee et al., 2006).

Several anthropogenic substances that can yield SOA are known, but not included in the model either for lack of

Table 4. Model estimate of SOA precursor emission, SOA production and atmospheric burden. E: emissions ($Tg\,yr^{-1}$), P: aerosol production ($Tg\,yr^{-1}$), B: mean burden (Tg). Subscript i denotes precursor isoprene, t monoterpenes, a anthropogenics and tot total SOA.

Reference	Model	E_i	E_t	E_a	P_i	P_t	P_a	B_i	B_t	B_a	B_{tot}
Tsigaridis and Kanakidou (2007)	TM3	467	137	16	4.6	12	1.8	0.08	0.69	0.04	0.81
Hoyle et al. (2007)	OSLO CTM2	220	127	17	15	38	2.5	–	–	–	0.52
Henze et al. (2008)	GEOS-CHEM	461	121	19	14	8.7	3.5	0.45	0.22	0.08	0.75
Heald et al. (2008)	CAM3	496	43	16	19	3.7	1.4	–	–	–	0.59
This study	ECHAM5/HAM	460	89	17	17	4.0	5.6	0.70	0.06	0.07	0.83

emissions estimates, or because they are recent discoveries. It has long been known that alkanes can yield aerosol, but this has been observed for larger (in terms of carbon number) members of the alkanes group: EDGAR emissions estimates are given only for the group as a whole. Certain alkenes are also SOA precursors (Forstner et al., 1997; Kalberer et al., 2000). A recent discovery is that even the lightest non-methane hydrocarbon (acetylene, C_2H_2) can yield SOA (Volkamer et al., 2009). These compounds may go some way to explaining the large discrepancy between modelled and measured OC in anthropogenically-dominated regions.

Perhaps more importantly, seasonality is lacking in the emissions for primary organic particles as well as for anthropogenic SOA precursors. Other reasons may include lack of wood burning emissions, which may account for a substantial part of the observed organic mass at some locations (Simpson et al., 2007). This may play an important role in reconciling the model with observations over, for example, Southern Europe in wintertime.

5.1.2 SOA in the laboratory and in the real atmosphere

There are some critical differences between the worlds of laboratory experiment and global model. In laboratory experiments, SOA is generated from a single pulse of precursor gas, and the SOA yield measured at the end of the experiment. The time dimension that is the experiment duration is not of primary importance for the purpose. Neither is the fate of the gas-phase moiety of the semi-volatile species at the end of the measurement an important consideration. By contrast, in the atmosphere, precursors are supplied in a continuous flux (although this may be zero in some cases, such as isoprene at night). Experiments are necessarily time-limited (typically not more than 12 h) due to factors including wall losses and the need to obtain accurate measurements. In the atmosphere, both aerosol and gas continue to evolve. The gas phase condensable species produced cannot be ignored, since, as long as they are present in the atmosphere, they may ultimately condense to form new aerosol mass. Kroll and Seinfeld (2008) discuss requirements for a more complete representation of semi-volatile species, including:

1. Direct removal from the gas phase through wet and dry deposition
2. Condensation to the aerosol phase and removal from there
3. Chemical transformation, which may yield either more (through breaking of the carbon chain) or less (through addition of oxygen) volatile species

The removal processes (1) and (2) are represented in this model, although there is considerable uncertainty in the choice of physical properties (solubility, molecular weight) of the model compounds.

The lack of any chemical aging process is potentially more serious. The very large contribution of isoprene-derived SOA product 1 to high altitude aerosol has been discussed in chapter 3.4. If this product were subject to reactions that yield only lighter, pure gas phase products, then clearly the final SOA burden can only be reduced. If instead it were subject to reactions that yield less volatile products, then competing effects upon aerosol mass would result. On one hand, it would increase the proportion of mass found in the aerosol phase; on the other, a greater proportion of the aerosol could condense at lower altitudes, where liquid water can exist, thereby strengthening the wet deposition sink, leaving the overall effect unclear.

The effect of NO_x on production of SOA from isoprene (Kroll et al., 2006), monoterpenes (Ng et al., 2007a, b), and aromatic compounds (Henze et al., 2008) is well documented. These results indicate a reduced SOA yield under high NO_x for all species that are included in this model. This may be of particular importance for anthropogenic species, since NO_x is mainly anthropogenic, and therefore high NO_x levels and high anthropogenic SOA levels are expected to coincide. Omission of the effect of NO_x might, accordingly, be expected to cause an overestimate of anthropogenic SOA yields. However, as we have seen for isoprene SOA, volatile gases that produce little aerosol mass near the surface may produce substantial aerosol mass higher in the atmosphere, so that one cannot draw any firm conclusions on the overall effect of NO_x on SOA production.

5.2 Optical properties of SOA

Some studies of the optical properties of SOA exist (e.g. Dinar et al., 2008), but fall short of what the model requires for computation of radiative properties, namely complex refractive index measured at several wavelengths for a representative selection of substances occurring in real SOA. Organic aerosols are known to be primarily scattering, but some species exhibit significant absorption in the ultra-violet (Myrhe and Nielsen, 2004). In this study, the same optical properties as POA have been assumed (Stier et al., 2005).

5.3 Nucleation and growth of small particles

In this model, SOA only condenses upon existing particles. Nucleation of new particles is determined by sulphuric acid and water, without reference to organic substances. Recent laboratory studies have shown that nucleation can occur through homogenous nucleation of sulphuric acid (Sipilä et al., 2010) or through heterogenous nucleation of sulphuric acid and organic vapours (Metzger et al., 2010). That the latter mechanism is important in the atmosphere is confirmed by observations (e.g. O'Dowd et al., 2002; Smith et al., 2008) of organic compounds in ultrafine particles. The lack of any organic compound in the nucleation mode means that SOA cannot condense onto nucleation mode particles. SOA is therefore unable to drive the growth of small particles, which has been observed in certain environments (for example, Kulmala et al., 2004; Laaksonen et al., 2008). Furthermore, laboratory studies have identified mechanisms whereby organics evolve chemically in the aerosol phase. These include heterogenous reactions leading to the formation of organic oligomers (in certain cases acid-catalysed) and of organosulphates (Wang et al., 2010; Hallquist et al., 2009, and the references therein). The products of such reactions include low-volatility compounds. The simple thermodynamic phase partitioning scheme as employed in this model is not capable of reflecting these processes. For these reasons, it is likely that the model underestimates the organic contribution to small particles.

5.4 Vertical distribution, cloud processing and SOA lifetime

It has been noted in chapter 3.4 that the vertical distribution of SOA, in particular the biogenic distribution, where the products are assumed semi-volatile, is very substantially affected by the volatility of the compound in question. One may question if the laboratory data chosen to represent isoprene, in particular, are suitable to apply throughout the troposphere for atmospheric studies. There are few published estimates of the two-product parameters that described isoprene-derived SOA (Carlton et al., 2009 and the references therein), but all share the same characteristic high stoichiometric coefficient (α_1) and low partitioning coefficient ($K_{p,1}$), for one of the products.

Vertical distribution is also dependent upon aerosol aging processes and interactions with clouds. In this model, no SOA aging processes exist, and the only interaction with clouds is the wet scavenging of aerosols and gases.

In the last decade, a great deal of effort has been put into understanding the chemical pathways of SOA formation. Unfortunately, comparatively little effort has been expended in characterising sink processes of SOA. Information about the properties that govern the efficiency of the main sink process, wet deposition, is completely lacking. In order to calculate wet deposition from the gas phase of any species, one must know the Henry's Law coefficient for that species. In this study, coefficients have been chosen from http://www.mpch-mainz.mpg.de/~sander/res/henry.html among many possible choices among the products of SOA precursor oxidation. The two-product model thus creates a paradox, whereby the volatility of a wide spectrum of real compounds is represented by two fictitious compounds: yet a complete model requires several physical parameters that must be assigned to the two fictitious compounds using the properties of real compounds.

5.5 Direct and indirect effects of SOA

Yu et al. (2006) surveyed model studies of direct radiative effect of several models and compared them against satellite-derived observational estimates. SOA is not explicitly included in any of the models (which do not include ECHAM5-HAM). The observation-based median estimate of DRE is $-5.9\,\mathrm{Wm}^{-2}$ and that of the models $-2.8\,\mathrm{Wm}^{-2}$.

The modelled SOA direct effect over land is $-0.35\,\mathrm{Wm}^{-2}$ and over ocean $-0.29\,\mathrm{Wm}^{-2}$, so that SOA accounts for a sizeable fraction of the model-observation discrepancy. Other reasons for the discrepancy may include the unavailability of satellite observations over high-albedo surfaces such as snow, ice and low clouds, where the true direct effect may even be positive (Quaas et al., 2008).

Forster et al. (2007) compared direct radiative forcing of several models against three satellite-derived estimates. Again, the satellite-derived results indicate a higher direct forcing than is modelled.

Finally, one can note that Forster et al. (2007) found a direct radiative forcing of just $-0.05\,\mathrm{Wm}^{-2}$ for OC from fossil fuel. In this light, the estimated radiative effect of SOA may appear large. However, one must bear in mind that the modelled vertical distribution and lifetime of SOA are completely different from those of POA, and that its mixing state and size distribution are also very different, since it is mostly of biogenic origin and therefore not related to black carbon.

Model estimates of the global cloud albedo effect range from $-0.5\,\mathrm{Wm}^{-2}$ to $-1.9\,\mathrm{Wm}^{-2}$in the models surveyed by Lohmann and Feichter (2005). In recent years, relationships have been derived between satellite retrievals of cloud

properties and aerosol optical depth (Quaas et al., 2008 and the references therein) and used to constrain models. The results indicate that earlier model studies overestimate the cloud albedo effect. Quaas et al. (2008) estimate the cloud albedo effect to be $-0.2 \pm 0.1\,\mathrm{Wm}^{-2}$. Possible contributors to the model overestimates include the model parameterisation of the autoconversion rate (i.e. the rate of conversion of cloud droplets to raindrops) and whether the model cloud updraft velocity depends on the turbulent kinetic energy (Forster et al., 2007).

This study identifies another possible source of overestimate: secondary organic aerosols. In chapter 3.7, it was shown that, in some regions, the CCN concentration may be decreased by SOA (although this result does depend on the model definition of CCN as any particle of radius $>35\,\mathrm{nm}$). Note that only a model with size-resolved aerosol microphysics can produce this effect, and that it might not occur in models using other cloud droplet activation schemes. Whether this SOA impact is a reasonable reflection of real cloud processes is not possible to state with any certainty, but since (i) it reduces the gap between estimates by model alone and observationally constrained estimates and (ii) the cloud decks affected in the model are observed to be susceptible to aerosol modification (Quaas et al., 2008), some encouragement may be taken from the results.

5.6 Model results and surface observations

Comparison of modelled total organic aerosol concentration to surface observations yields mixed results. On the positive side, there is a clear improvement in agreement between model and measurements at the IMPROVE network, but the failure of the model to capture either the observed magnitude of POM or its seasonal variability at the southern European EMEP sites remains a major concern, as is the fact that the model remains systematically too low on organic mass compared to nearly all measurements.

Possible reasons for the remaining discrepancies include:

1. Constant anthropogenic emissions. Neither POA nor anthropogenic SOA precursor emissions in the model have either a diurnal or a seasonal cycle. For SOA precursors, night-time emissions are not subject to photochemical conversion by OH. Transport is a major user of fossil fuels, and much more of this takes place during the day. Heating and lighting requirements for fossil fuels are also greater in winter. A single annual emission flux, applied throughout each day and throughout the year, is unrealistic.

2. Missing SOA precursors. SOA precursors, both anthropogenic and biogenic, are known but have not been included in the model either for lack of emission inventories or laboratory data that can quantify the SOA yield and volatility from that precursor.

3. Missing primary organic semi-volatile substances (Robinson et al., 2007).

4. Intermediate compounds. By this is meant compounds that are short-lived but can partition to the aerosol phase. In a smog chamber experiment, where the precursor gas is injected in a single pulse, such compounds will die out quickly, possibly taking no part in the aerosol measurement at the end of the experiment. In the atmosphere, such compounds will be replaced in a continuous flux (Galloway et al., 2009)

5. Missing particle and aqueous phase chemistry.

6. Adsorptive uptake of SOA.

7. Lack of wood burning emissions, which may account for a substantial part of the observed organic mass at some locations (Simpson et al., 2007).

6 Summary and conclusions

Secondary organic aerosol (SOA) has been introduced into the global aerosol-climate model ECHAM5-HAM. The SOA submodel treats both anthropogenic and biogenic sources of SOA. Anthropogenic precursor gases include toluene, xylene and benzene. Emissions of anthropogenic precursors are prescribed. Biogenic precursor gases included in the model are isoprene and monoterpenes. Monoterpene species are lumped together, using the properties of α-pinene as a surrogate. Biogenic emissions are calculated online, depending on temperature and leaf area index (for both isoprene and monoterpenes) as well as photosynthetically active radiation (for isoprene), following the widely used parameterisations of Guenther et al. (2006) and Guenther et al. (1995).

The model calculates SOA formation from the precursor gases using a highly simplified chemistry scheme, with prescribed monthly values for the concentrations of OH, O_3 and NO_3. Only the major SOA production for each precursor is considered to form SOA (ozonolysis of monoterpenes, and OH oxidation for all other species). The two-product model of SOA formation developed by Odum et al. (1996), extended as described in the Appendix for distinct size classes, is used to calculate gas-aerosol phase partitioning..

The SOA submodel takes advantage of the tracer transport, convection and diffusion processes of ECHAM and the aerosol microphysics and gas and aerosol sink processes of HAM. The HAM aerosol radiation module permits size- and composition-resolved calculation of the radiative influence of aerosols. In order to allow for hygroscopic growth of organic aerosols, a new water uptake parameterisation (Petters and Kreidenweis, 2007) has been implemented.

The results of two simulations, where the large-scale climate was constrained by nudging to the same reference meteorology, one simulation with SOA and one without, are presented and compared.

Calculated biogenic emissions under year 2000 conditions are 446 Tg yr^{-1} isoprene and 89 Tg yr^{-1} monoterpenes. Emisson of anthropogenic SOA precursors amounts to 17 Tg yr^{-1}. Aerosol production is estimated as 21 Tg yr^{-1} from biogenic sources and 5.6 Tg yr^{-1} from anthropogenic precursors. This compares with 47 Tg POA emissions and 71 Tg sulphate aerosol production.

Column burdens of SOA are highest over the source regions, with biogenic SOA present especially over the tropical forests of Africa and South America. Anthropogenic SOA is largest over the Indian subcontinent, due to high benzene emissions. The modelled atmospheric lifetimes of SOA derived from anthropogenic precursors and from monoterpenes, at 4.8 days and 5.8 days respectively, are comparable to those of other fine-mode aerosol species (e.g. sulphate, 4.6 days; POA 6.0 days); but for isoprene-derived SOA, the lifetime reaches over 15 days. This has been shown to be a result of the laboratory data describing the SOA yield from isoprene oxidation in terms of the two-product model. One such product is described as being produced with a high yield, but highly volatile, favouring condensation to the aerosol phase only at very low temperatures. This leads to large amounts of SOA condensing in the upper troposphere, to which the gas-phase semi-volatiles are transported by tropical convection. At altitudes too cold for liquid water, sinks of SOA (which, in the model, does not interact with cloud ice) are very weak, which leads to the extended atmospheric lifetime.

Aerosol optical depth increases only modestly due to SOA, increasing the global annual mean AOD by just 0.01. Regionally and seasonally, the increase in AOD can be much larger, with increases of up to 0.2 modelled for the Amazon region in the biomass burning season.

A comparison of model results against measurements has been performed, with the emphasis on wide area and longer term (measurement data over one year were used), with the aim of evaluating the distribution of model results against that of the measurements, rather than concentrating on point-by-point comparison of single stations or short field campaigns. Comparison of simulated total organic aerosol concentration against the IMPROVE network of rural stations in the United States showed significantly better agreement with the simulation including SOA, especially in the summer months. For a network of stations in western and central Europe, the model performance was poorer, especially southern Europe. Analysis of correlation between measured organic and elemental carbon (a marker of anthropogenic activity) showed that times and places of poorest model performance are strongly dominated by anthropogenic OC. Whether this is primary or secondary material is not known. In general, the model underestimates organic aerosol mass. While the underestimation is reduced in the simulation with SOA, it is clear that the SOA species included for in the model do not account for all the "missing" OC. Comparison of modelled AOD values against measurements from the AERONET network showed a modest improvement in the simulation with SOA, but again the modelled values remain systematically too low.

Finally, estimates of the direct and indirect effects of SOA have been presented. The direct SW radiative effect of SOA is estimated as $-0.31\,\mathrm{Wm}^{-2}$, concentrated over the biogenic source regions. The indirect SW effect is, surprisingly, positive, amounting to $+0.23\,\mathrm{Wm}^{-2}$. Analysis of the distribution of particles that can act as cloud condensation nuclei (CCN) shows that the model SOA can act to increase or to decrease CCN. In pristine areas, condensation of SOA boosts growth of small particles, increasing CCN. However in polluted areas, where particles are present in sufficient numbers, the stronger effect is the strengthening of the coagulation sink as particles grow larger, decreasing CCN. In such areas, SOA acts to counteract the indirect effect of anthropogenic aerosols, leading to the positive radiative effect. LW radiative effects are estimated to be close to zero: the net result of all effects is a weak net cooling of $-0.09\,\mathrm{Wm}^{-2}$.

The model development herein described represents a second step in modelling of atmospheric organic aerosols, a vast and diverse array of compounds (the first step being the modelling of primary organic particles). Subsequent steps may include the addition of further SOA precursors as laboratory data and emission inventories allow; integration of the scheme with a fully-featured atmospheric chemistry model; development of further chemistry of SOA formation, which may include particle phase, aqueous and acid-catalysed reactions; atmospheric aging of SOA; parameterisation of the role of SOA in new particle nucleation and possibly interaction with cloud ice, when knowledge of those processes reaches a sufficient level. Although much progress has been made in recent years, the path to a sound level of scientific understanding of atmospheric organic particles remains a long one.

Appendix A

Gas-aerosol partitioning

A1 Total (bulk) gas-aerosol partitioning

Pankow (1994a) derived an expression for the partitioning coefficient $K_{p,i}$ in terms of temperature and aerosol solution properties, here presented in the slightly modified form of Seinfeld and Pankow (2003), and in terms of SI units:

$$K_{p,i} = \frac{\mathrm{RT}}{\mathrm{MW_{OM}}\zeta_i p_i^0} \tag{A1}$$

where $\mathrm{MW_{OM}}$ is the mean molecular weight of the organic aerosol, R the universal gas constant, T the temperature, ζ_i the activity coefficient of compound i and p_i^0 its saturation vapour pressure. We take the activity coefficient of each compound to be unity. The Clausius-Clapeyron equation for the temperature dependence of p_i^0 applied to Eq. (A1) then

allows us to calculate $K_{p,i}$ at any temperature from that at a reference temperature T_{ref}, where the partitioning coefficient is $(K_{p,i})_{\mathrm{ref}}$:

$$K_{p,i} = \left(K_{p,i}\right)_{\mathrm{ref}} \frac{T}{T_{\mathrm{ref}}} \exp\left[\frac{\Delta H_i}{R}\left(\frac{1}{T} - \frac{1}{T_{\mathrm{ref}}}\right)\right] \quad \text{(A2)}$$

where ΔH_i is the enthalpy of vaporisation of compound i. ΔH_i is set to 42 kJ mol^{-1} for all semivolatile species in this model.

In this model, SOA partitioning is calculated independently of SOA formation. SOA is transported and can evaporate or condense as ambient conditions vary.

Where S_i is the total mass of semi-volatile SOA species i, and A_i and G_i its aerosol and gas phase masses respectively, then

$$S_i = A_i + G_i \quad \text{(A3)}$$

Equilibrium of the total is given by (3); to reiterate,

$$A_i = K_{p,i} M_0 G_i \quad \text{(A4)}$$

Substituting from Eq. (A3) and rearranging gives

$$G_i = \frac{S_i}{1 + K_{p,i} M_0}, \text{and} \quad \text{(A5)}$$

$$A_i = \frac{K_{p,i} M_0 S_i}{1 + K_{p,i} M_0} \quad \text{(A6)}$$

Thus the SOA absorbing mass M_0 must be known before the partitioning can be calculated, although it is itself a function of the SOA aerosol mass. Recalling that M_0 consists of a non-volatile part M_{NV} (which in this model consists of POA and non-volatile SOA), plus all condensed SOA,

$$M_0 = M_{\mathrm{NV}} + \sum_i A_i \quad \text{(A7)}$$

Substituting from Eq. (A6), we have finally

$$M_0 = M_{\mathrm{NV}} + M_0 \sum_{i=1}^{n} \frac{K_{p,i} S_i}{1 + K_{p,i} M_0} \quad \text{(A8)}$$

Thus, since the total non-volatile and semi-volatile masses M_{NV} and S_i are known, we can compute M_0 and thence the gas and aerosol phase masses of the semi-volatile species.

Equation (A8) and the foregoing equations have been stated in many previous works (e.g. Seinfeld and Pankow, 2003; Tsigaridis and Kanakidou, 2003; Hoyle et al., 2007).

A2 Gas-aerosol partitioning per mode

Repeating the derivation of Pankow (1994a, b), under the assumption that there exists a partitioning coefficient $K_{p,i,j}$ for species i in each mode j, results in a similar expression to Eq. (A1)

$$K_{p,i,j} = \frac{\mathrm{RT}}{\mathrm{MW}_{\mathrm{OM},j} \zeta_{i,j} p_i^0} \quad \text{(A9)}$$

where $\mathrm{MW}_{\mathrm{OM},j}$ is the mean molecular weight of the organic species in mode j, and $\zeta_{i,j}$ the activity coefficient for species i the mode. The ratio of mode to bulk partitioning coefficient is then

$$\frac{K_{p,i,j}}{K_{p,i}} = \frac{\mathrm{MW}_{\mathrm{OM}} \zeta_i}{\mathrm{MW}_{\mathrm{OM,j}} \zeta_{i,j}} \quad \text{(A10)}$$

Since the activity coefficients are taken to be unity for all modes, only the ratio of the mean molecular weights remains, for which unity is a reasonable assumption. Then the bulk partitioning coefficient can be used for all modes.

Now suppose we have two sets of numbers x_i and y_i such that the ratio of each pair of numbers is the same.

$$\frac{x_i}{y_i} = k \quad \text{(A11)}$$

where k is a constant, then

$$\frac{x_i + x_j}{y_i + y_j} = \frac{k y_i + k y_j}{y_i + y_j} = k \quad \text{(A12)}$$

This can be iterated as many times as we wish, so that we can write

$$\frac{\sum_{i=1}^{n} x_i}{\sum_{i=1}^{n} y_i} = k \quad \text{(A13)}$$

Now consider semi-volatile aerosol of different size classes (modes) in phase equilibrium. Let A_{ij} denote the mass concentration of species i in mode j, $M_{\mathrm{NV}j}$ and M_{0j} the mass concentrations of non-volatile SOA absorbers and total SOA absorbers respectively in mode j. Let A_i, M_{NV} and M_0 be the corresponding total quantities. G_i is the gas-phase masss concentration of species i and $K_{p,i}$ its partitioning coefficient.

Equilibrium of each mode specifies the same gas phase, and further, it has been shown that the same partitioning coefficient may be used for all size modes. Then

$$A_{ij} = K_{p,i} M_{0j} G_i \quad \text{(A14)}$$

The fraction of SOA species i in mode j is, by dividing Eq. (A14) by Eq. (A13):

$$\frac{A_{ij}}{A_i} = \frac{M_{0j}}{M_0} \quad \text{(A15)}$$

Observe that the right hand side is independent of i, so Eq. (A15) is true for all i. Because the ratio of A_{ij} to A_i is the same for all i for a given j, we can, following Eqs. (A11)–(A13), write

$$\frac{A_{ij}}{A_i} = \frac{\sum_{i=1}^{n} A_{ij}}{\sum_{i=1}^{n} A_i} \quad \text{(A16)}$$

Substituting Eq. (A16) in the left hand side of Eq. (A15) and expanding the M_0 terms on the right hand side of Eq. (A15) into their non-volatile and semi-volatile components using Eq. (A7)

$$\frac{\sum_{i=1}^{n} A_{ij}}{\sum_{i=1}^{n} A_i} = \frac{M_{\mathrm{NV}j} + \sum_{i=1}^{n} A_{ij}}{M_{\mathrm{NV}} + \sum_{i=1}^{n} A_i} \tag{A17}$$

The product of sums terms cancel on cross-multiplying, leaving

$$\frac{\sum_{i=1}^{n} A_{ij}}{\sum_{i=1}^{n} A_i} = \frac{M_{\mathrm{NV}j}}{M_{\mathrm{NV}}} \tag{A18}$$

Or, using Eq. (A16) again,

$$\frac{A_{ij}}{A_i} = \frac{M_{\mathrm{NV}j}}{M_{\mathrm{NV}}} \tag{A19}$$

Acknowledgements. The authors wish to thank John H. Seinfeld, Philip Stier, Daven Henze, Sally Ng, and Havela Pye for their valuable input and helpful discussions.

The service charges for this open access publication have been covered by the Max Planck Society.

Edited by: V.-M. Kerminen

References

Andreae, M. O. and Crutzen, P. J.: Atmospheric Aerosols: Biogeochemical Sources and Role in Atmospheric Chemistry, Science, 276, 1052–1058, 1997.

Arneth, A., Monson, R. K., Schurgers, G., Niinemets, Ü., and Palmer, P. I.: Why are estimates of global terrestrial isoprene emissions so similar (and why is this not so for monoterpenes)?, Atmos. Chem. Phys., 8, 4605–4620, doi:10.5194/acp-8-4605-2008, 2008.

Artaxo, P., Storms, H., Bruynseels, F., and Van Greiken, R.: Composition and Sources of Aerosols From the Amazon Basin, J. Geophys. Res., 93(D2), 1605–1615, doi:10.1029/JD093iD02p01605, 1988.

Artaxo, P., Martins, J. V., Yamasoe M. A., Procópio, A. S., Pauliquevis, T. M., Andreae, M. O., Guyon, P., Gatti L. V., and Cordova Leal, A. M.: Physical and chemical properties of aerosols in the wet and dry seasons in Rondônia, Amazonia, J. Geophys. Res., 107(D20), 8081, doi:10.1029/2001JD000666, 2002.

Baltensperger, U., Kalberer, M., Dommen, J., Paulsen, D., Alfarra, M. R., Coe, H., Fisseha, R., Gascho, A., Gysel, M., Nyeli, S., Sax, M., Steinbacher, M., Prévot, A. S. H., Sjögren, S. Weingartner, E., and Zenobi, R.: Secondary organic aerosols from anthropogenic and biogenic precursors, Faraday Discuss. 130, 265–278, 2005.

Bonn, B. and Moortgat, G. K.: Sesquiterpene ozonolysis: Origin of atmospheric new particle formation from biogenic hydrocarbons, Geophys. Res. Lett., 30(11), 1585, doi:10.1029/2003GL017000, 2003.

Bonn, B., Kulmala, M., Riipinen, I., Sihto, S.-L., and Ruuskanen, T. M.: How biogenic terpenes govern the correlation between sulfuric acid concentrations and new particle formation, J. Geophys. Res., 113, D12209, doi:10.1029/2007JD009327, 2008.

Carlton, A. G., Wiedinmyer, C., and Kroll, J. H.: A review of Secondary Organic Aerosol (SOA) formation from isoprene, Atmos. Chem. Phys., 9, 4987–5005, doi:10.5194/acp-9-4987-2009, 2009.

Carlton, A. G., Pinder, R. W., Bhave, P. V., and Pouliot, G. A.: To what extent can biogenic SOA be controlled?, Environ. Sci. Technol. 44(9), 3376–3380, 2010.

Chung, S. H. and Seinfeld, J. H.: Global distribution and climate forcing of carbonaceous aerosols, J.Geophys. Res., 107(D19), 4407, doi:10.1029/2001JD001397, 2002.

Dentener, F., Kinne, S., Bond, T., Boucher, O., Cofala, J., Generoso, S., Ginoux, P., Gong, S., Hoelzemann, J. J., Ito, A., Marelli, L., Penner, J. E., Putaud, J.-P., Textor, C., Schulz, M., van der Werf, G. R., and Wilson, J.: Emissions of primary aerosol and precursor gases in the years 2000 and 1750 prescribed data-sets for AeroCom, Atmos. Chem. Phys., 6, 4321–4344, doi:10.5194/acp-6-4321-2006, 2006.

Dinar, E., Abo Riziq, A., Spindler, C., Erlick, C., Kiss, G., and Rudich, Y.: The complex refractive index of atmospheric and model humic-like substances (HULIS) retrieved by a cavity ring down aerosol spectrometer (CRD-AS), Faraday Discuss. 137, 279–295, 2008

Forstner, H. J. L., Seinfeld, J. H., and Flagan, R. C.: Molecular speciation of secondary organic aerosol from the higher alkenes: 1-octene and 1-decene, Atmos. Environ. 31, 1953–1964, 1997.

Forster, P., Ramaswamy, V., Artaxo, P., Berntsen, T., Betts, R., Fahey, D. W., Haywood, J., Lean, J., Lowe, D. C., Myhre, G., Nganga, J., Prinn, R., Raga, G., Schulz, M., and van Dorland, R.: Changes in Atmosperic Constituents and Radiative Forcing, in: Climate Change 2007:The Physical Science Basis. Contribution of Working Group I to the Intergovernmental Panel on Climate Change, edited by: [Solomon, S., Qin, D., Manning, M., Chen, D., Marquis, M., Averyt, K. B., Tignor M., and Miller, H. L., Cambridge University Press, Cambridge, United Kingdom and New York, NY, USA, 2007.

Froyd, K. D., Murphy, D. M., Sanford, T. J., Thomson, D. S., Wilson, J. C., Pfister, L., and Lait, L.: Aerosol composition of the tropical upper troposphere, Atmos. Chem. Phys., 9, 4363–4385, doi:10.5194/acp-9-4363-2009, 2009.

Galloway, M. M., Chhabra, P. S., Chan, A. W. H., Surratt, J. D., Flagan, R. C., Seinfeld, J. H., and Keutsch, F. N.: Glyoxal uptake on ammonium sulphate seed aerosol: reaction products and reversibility of uptake under dark and irradiated conditions, Atmos. Chem. Phys., 9, 3331–3345, doi:10.5194/acp-9-3331-2009, 2009.

Ganzefeld, L. and Lelieveld, J.: Dry deposition parameterization in a chemistry general circulation model and its influence on the distribution of reactive trace gases, J. Geophys. Res., 100, 20999–21012, doi:10.1029/95JD02266, 1995.

Ganzeveld, L., Lelieveld, J., and Roelofs, G.-J.: Dry deposition parameterization of sulfur oxides in a chemistry and gen-

eral circulation model, J. Geophys. Res., 103, 5679–5694, doi:10.1029/97JD03077, 1998.

Guenther, A.: Corrigendum to "Estimates of global terrestrial isoprene emissions using MEGAN (Model of Emissions of Gases and Aerosols from Nature)" published in Atmos. Chem. Phys., 6, 3181-3210, 2006, Atmos. Chem. Phys., 7, 4327–4327, doi:10.5194/acp-7-4327-2007, 2007.

Guenther, A., Hewitt, C., Erickson, D., Fall, R., Geron, C., Graedel, T., Harley, P., Klinger, L., Lerdau, M., McKay, W., Pierce, T., Scholes, B., Steinbrecher, R., Tallamraju, R., Taylor, J., and Torres, L.: A global model of natural volatile organic compound emissions, J. Geophys. Res., 100, 8873–8892, doi:10.1029/94JD02950, 1995.

Guenther, A., Karl, T., Harley, P., Wiedinmyer, C., Palmer, P. I., and Geron, C.: Estimates of global terrestrial isoprene emissions using MEGAN (Model of Emissions of Gases and Aerosols from Nature), Atmos. Chem. Phys., 6, 3181–3210, doi:10.5194/acp-6-3181-2006, 2006.

Hallquist, M., Wenger, J. C., Baltensperger, U., Rudich, Y., Simpson, D., Claeys, M., Dommen, J., Donahue, N. M., George, C., Goldstein, A. H., Hamilton, J. F., Herrmann, H., Hoffmann, T., Iinuma, Y., Jang, M., Jenkin, M. E., Jimenez, J. L., Kiendler-Scharr, A., Maenhaut, W., McFiggans, G., Mentel, Th. F., Monod, A., Prévôt, A. S. H., Seinfeld, J. H., Surratt, J. D., Szmigielski, R., and Wildt, J.: The formation, properties and impact of secondary organic aerosol: current and emerging issues, Atmos. Chem. Phys., 9, 5155–5236, doi:10.5194/acp-9-5155-2009, 2009.

Heald, C. L., Jacob, D. J., Park, R. J., Russell, L. M., Huebert, B. J., Seinfeld, J. H., Liao, H., and Weber, R. J.: A large organic aerosol source in the free troposphere missing from current models, Geophys. Res. Lett., 32, L18809, doi:10.1029/2005GL023831, 2005.

Heald, C. L., Henze, D. K., Horowitz, L. W., Feddema, J., Lamarque, J.-F., Geunther, A., Hess, P. G., Vitt, F., Seinfeld, Goldstein, A. H., and Fung, I.: Predicted change in global secondary organic aerosol concentration in response to future climate, emissions and land use change, J. Geophys. Res. 113, D05211, doi:10.1029/2007JD009092, 2008.

Hegg, D. A., Livingston, J., Hobbs, P. V., Novakov, T., and Russell, P.: Chemical apportionment of aerosol column optical depths off the mid-Atlantic coast of the United States, J. Geophys. Res., 102, 25293–25303, doi:10.1029/97JD02293, 1997.

Henze, D. K. and Seinfeld, J. H.: Global secondary organic aerosol from isoprene oxidation, Geophys. Res. Lett., 33, L09812, doi:10.1029/2006GL025976, 2006.

Henze, D. K., Seinfeld, J. H., Ng, N. L., Kroll, J. H., Fu, T.-M., Jacob, D. J., and Heald, C. L.: Global modeling of secondary organic aerosol formation from aromatic hydrocarbons: high-vs. low-yield pathways, Atmos. Chem. Phys., 8, 2405–2420, doi:10.5194/acp-8-2405-2008, 2008.

Holben, B. N., Eck, T. F., Slutsker, I., Tanré, D., Buis, J. P., Setzer, A., Vermote, E., Reagan, J. A., Kaufman, Y. J., Nakajima, T., Lavenu, F., Jankowiak, I., and Smirnov, A.: AERONET – A Federated Instrument Network and Data Archive for Aerosol Characterization, Remote Sens. Environ., 66, 1–16, 1998.

Hoffmann, T., Odum, J. R., Bowman, F., Collins, D., Klockow, D., Flagan, R. C., and Seinfeld, J. H.: Formation of organic aerosols from the oxidation of biogenic hydrocarbons, J. Atmos. Chem., 26, 189–222, 1997.

Hoyle, C. R., Berntsen, T., Myhre, G., and Isaksen, I. S. A.: Secondary organic aerosol in the global aerosol - chemical transport model Oslo CTM2, Atmos. Chem. Phys., 7, 5675–5694, doi:10.5194/acp-7-5675-2007, 2007.

Hoyle, C. R., Myhre, G., Berntsen, T. K., and Isaksen, I. S. A.: Anthropogenic influence on SOA and the resulting radiative forcing, Atmos. Chem. Phys., 9, 2715–2728, doi:10.5194/acp-9-2715-2009, 2009.

Huebert, B., Bertram, T., Kline, J., Howell, S., Eatough, D., and Blomquist, B.: Measurements of organic and elemental carbon in Asian outflow during ACE-Asia from the NSF/NCAR C-130, J. Geophys. Res. 109, D19S11, doi:10.1029/2004JD004700, 2004.

Iinuma, Y., Böge, O., Gnauk, T., and Herrmann, H.: Aerosol-chamber study of the α-pinene/O_3 reaction: Influence of particle acidity on aerosol yields and products, Atmos. Environ. 38, 761–773, 2004.

Jacobson, M. Z., Tabadazeh, A., and Turco, R. P.: Simulating equilibrium within aerosols and nonequilibrium between gases and aerosols, J. Geophys. Res., 101(D4), 9079–9091, doi:10.1029/96JD00348, 1996.

Kalberer, M., Yu, J., Cocker, D. R., Flagan, R. C., and Seinfeld, J. H.: Aerosol formation in the cyclohexene-ozone system, Environ. Sci. Technol., 34 4894–4901, 2000.

Kroll, J. H. and Seinfeld, J. H.: Chemistry of secondary organic aerosol: Formation and evolution of low-volatility organics in the atmosphere, Atmos. Environ., 42, 3593–3624, 2008.

Kroll, J. H., Ng, N. L., Murphy, S. M., Flagan, R. C., and Seinfeld, J. H.:, Secondary Organic Aerosol Formation from Isoprene Photooxidation, Environ. Sci. Technol., 40, 1869–1877, 2006.

Kulmala, M., Vehkamäki, H., Petäjä, T., Dal Maso, M., Lauri, A., Kerminen,V.-M., Birmili, W., and McMurry, P. H.: Formation and growth rates of ultrafine atmospheric particles: a review of observations, J. Aerosol Sci., 35(2), 143–176, 2004.

Kulmala, M., Reissell, A., Sipila, M., Bonn, B., Ruuskanen, T. M., Lehtinenen, K. E. J., Kerminen, V.-M., and Strom, J.: Deep convective clouds as aerosol production engines: Role of insoluble organics, J. Geophys. Res., 111(D17), D17202, doi:10.1029/2005JD006963, 2006.

Laaksonen, A., Kulmala, M., O'Dowd, C. D., Joutsensaari, J., Vaattovaara, P., Mikkonen, S., Lehtinen, K. E. J., Sogacheva, L., Dal Maso, M., Aalto, P., Petäjä, T., Sogachev, A., Yoon, Y. J., Lihavainen, H., Nilsson, D., Facchini, M. C., Cavalli, F., Fuzzi, S., Hoffmann, T., Arnold, F., Hanke, M., Sellegri, K., Umann, B., Junkermann, W., Coe, H., Allan, J. D., Alfarra, M. R., Worsnop, D. R., Riekkola, M.-L., Hyötyläinen, T., and Viisanen, Y.: The role of VOC oxidation products in continental new particle formation, Atmos. Chem. Phys., 8, 2657–2665, doi:10.5194/acp-8-2657-2008, 2008.

Lee, L., Goldstein, A. H., Kroll, J. H., Ng, N. L., Varutbangkul, V., Flagan, R. C., and Seinfeld, J. H.: Gas-phase products and secondary aerosol yields from the photooxidation of 16 different terpenes J. Geophys. Res. 111, D17305, doi:10.1029/2006JD007050, 2006.

Lin, H. and Leaitch, R.: Development of an in-cloud aerosol activation parameterization for climate modelling, in WMO workshop on measurement of cloud properties for forecasts of weather, pp. 328–225, World Meteorological Organisation, Geneva, 1997.

Lohmann, U. and Feichter, J.: Global indirect aerosol effects: a re-

view, Atmos. Chem. Phys., 5, 715–737, doi:10.5194/acp-5-715-2005, 2005.

Lohmann, U., Stier, P., Hoose, C., Ferrachat, S., Kloster, S., Roeckner, E., and Zhang, J.: Cloud microphysics and aerosol indirect effects in the global climate model ECHAM5-HAM, Atmos. Chem. Phys., 7, 3425–3446, doi:10.5194/acp-7-3425-2007, 2007.

Lund Myhre, C. E. and Nielsen, C. J.: Optical properties in the UV and visible spectral region of organic acids relevant to tropospheric aerosols, Atmos. Chem. Phys., 4, 1759–1769, doi:10.5194/acp-4-1759-2004, 2004.

Metzger, A., Verheggen, B., Dommen, J., Duplissy, J., Prevot, A. S. H., Weingartner, E., Riipinen, I., Kulmala, M., Spracklen, D. K., Carslaw, K. S., and Baltensperger, U.: Evidence for the role of organics in aerosol particle formation under atmospheric conditions, P. Natl. Acad. Sci. USA, 107(15) 6646–6651, 2010.

Middlebrook, A. M., Murphy, D. M., and Thomson, D. S.: Observations of organic material in individual marine particles at Cape Grim during the First Aerosol Characterization Experiment (ACE-1), J. Geophys. Res., 103(D13), 16475–16483, doi:10.1029/97JD03719, 1998.

Morgan, W. T., Allan, J. D., Bower, K. N., Capes, G., Crosier, J., Williams, P. I., and Coe, H.: Vertical distribution of sub-micron aerosol chemical composition from North-Western Europe and the North-East Atlantic, Atmos. Chem. Phys., 9, 5389–5401, doi:10.5194/acp-9-5389-2009, 2009.

Murphy, D. M., Thomson, D. S., and Mahoney, M. J.: In Situ Measurements of Organics, Meteoritic Material, Mercury and Other Elements in Aerosols at 5 to 19 Kilometers, Science, 282, 1664–1669, 1998.

Ng, N. L., Kroll, J. H., Chan, A. W. H., Chhabra, P. S., Flagan, R. C., and Seinfeld, J. H.: Secondary organic aerosol formation from *m*-xylene, toluene, and benzene, Atmos. Chem. Phys., 7, 3909-3922, doi:10.5194/acp-7-3909-2007, 2007a.

Ng, N. L., Chhabra, P. S., Chan, A. W. H., Surratt, J. D., Kroll, J. H., Kwan, A. J., McCabe, D. C., Wennberg, P. O., Sorooshian, A., Murphy, S. M., Dalleska, N. F., Flagan, R. C., and Seinfeld, J. H.: Effect of NO_x level on secondary organic aerosol (SOA) formation from the photooxidation of terpenes, Atmos. Chem. Phys., 7, 5159–5174, doi:10.5194/acp-7-5159-2007, 2007.

Novakov, T., Hegg, D. A., and Hobbs, P. V.: Airborne measurements of carbonaceous aerosols on the east coast of the United States J. Geophys. Res., 102, 30023–30030, 1997.

O'Dowd, C. D., Aalto, P., Hameri, K., Kulmala, M., and Hoffmann, T.: Aerosol formation – Atmospheric particles from organic vapours, Nature, 416, 497–498, 2002.

Odum, J. R., T. Hoffman, T., Bowman, F., Collins, D., Flagan, R. C., and Seinfeld, J. H.: Gas/Particle Partitioning and Secondary Organic Aerosol Yields, Environ. Sci. Technol., 30, 2580–2585, 1996.

Pankow, J. F.: An absorption model of gas/particle partitioning of organic compounds in the atmosphere, Atmos. Environ., 28(2), 185–188, 1994a.

Pankow, J. F.: An absorption model of the gas/particle partitioning involved in the formation of secondary organic aerosol, Atmos. Environ., 28(2), 189–193, 1994b.

Petters, M. D. and Kreidenweis, S. M.: A single parameter representation of hygroscopic growth and cloud condensation nucleus activity, Atmos. Chem. Phys., 7, 1961–1971, doi:10.5194/acp-7-1961-2007, 2007.

Presto, A. A., Huff Hartz, K. E., and Donahue, N. M.: Secondary Organic Aerosol Production from Terpene Ozonolysis 2. Effect of NO_x Concentration, Environ. Sci. Technol., 39, 7046–7054, 2005.

Pye, H. O. T. and Seinfeld, J. H.: A global perspective on aerosol from low-volatility organic compounds, Atmos. Chem. Phys., 10, 4377–4401, doi:10.5194/acp-10-4377-2010, 2010.

Olivier, J. G. J., van Aardenne, J. A., Dentener, F. J., Pagliari, V., Ganzeveld, L. N., and Peters, J. A. H. W.: Recent trends in global greenhouse gas emissions: regional trends 1970–2000 and spatial distribution of key sources in 2000, Environ. Sci. 2, 81–99, doi:10.1080/15693430500400345, 2005.

Quaas, J., Boucher, O., Bellouin, N., and Kinne, S.: Satellite-based estimate of the direct and indirect aerosol climate forcing, J. Geophys. Res., 113, D05204, doi:10.1029/2007JD008962, 2008.

Ramanathan, V., Crutzen, P. J., Lelieveld, J., Mitra, A. P., Althausen, D., Anderson, J., Andreae, M. O., Cantrell, W., Cass, G. R., Chung, C. E., Clarke, A. D., Coakley, J. A., Collins, W. D., Conant, W. C., Dulac, F., Heintzenberg, J., Heymsfield, A. J., Holben, B., Powell, S., Hudson, J., Jayaraman, A., Kiehl, J. T., Krishnamurti, T. N., Lubin, D., McFarquhar, G., Novakov, T., Ogren, J. A., Podgorny, I. A., Prather, K., Priestley, K., Prospero, J. M., Quinn, P. K., Rajeev, K., Rasch, P., Rupert, S., Sadourny, R., Satheesh, S. K., Shaw, G. E., Sheridan, P., and Valero, F. P. J.: Indian Ocean Experiment: An integrated analysis of the climate forcing and effects of the great Indo-Asian haze, J. Geophys. Res., 106(D22), 28371–28398, doi:10.1029/2001JD900133, 2001.

Robinson, A. L., Donahue, N. M., Shrivastava, M. K., Weitkamp, E. A., Sage, A. M., Grieshop, A. P., Lane, T. E., Pierce, J. R., and Pandis, S. N.: Rethinking organic aerosols: Semivolatile emissions and photochemical aging, Science, 315, 1259–1262, 2007

Roeckner, E., Bäuml G., Bonaventura, L., Brokopf, R., Esch, M., Giorgetta, M., Hagemann, S., Kirchner, I., Kornblueh, L., Manzini, E., Rhodin, A., Schlese, U., Schulzweida, U., Tompkins, A.: The atmospheric general circulation model ECHAM 5. PART I: Model description, MPI Report no. 349, available at: http://www.mpimet.mpg.de/fileadmin/publikationen/Reports/max_scirep_349.pdf, 2003.

Saathoff, H., Naumann, K.-H., Möhler, O., Jonsson, Å. M., Hallquist, M., Kiendler-Scharr, A., Mentel, Th. F., Tillmann, R., and Schurath, U.: Temperature dependence of yields of secondary organic aerosols from the ozonolysis of α-pinene and limonene, Atmos. Chem. Phys., 9, 1551–1577, doi:10.5194/acp-9-1551-2009, 2009.

Seinfeld, J. H. and Pankow, J. F.: Organic Atmospheric Particulate Material, Annu. Rev. Phys. Chem., 54, 121–140, 2003.

Simpson, D., Yttri, K.E., Klimont, Z., Kupiainen, K., Caseiro, A., Gelencsér, A., Pio, C., Puxbaum, H., and Legrand, M.: Modeling carbonaceous aerosol over Europe: Analysis of the CARBOSOL and EMEP EC/OC campaigns, J. Geophys. Res., 112, D23S14, doi:10.1029/2006JD008158, 2007.

Sipilä, M., Berndt, T., Petäjä, T., Brus, D., Vanhanen, J., Stratmann, F., Patokoski, J., Mauldin, R. L., Hyvärinen, A.-P., Lihavainen, H., and Kulmala, M.: The Role of Sulfuric acid in Atmospheric Nucleation, Science, 327, 1243–1246, 2010.

Smith, J. N., Dunn, M. J., VanReken, T. M., Iida, K., Stolzenburg, M. R., McMurry, P. H., and Huey, L. G.: Chemical compo-

sition of atmospheric nanoparticles formed from nucleation in Tecamac, Mexico: Evidence for an important role for organic species in nanoparticle growth, Geophys. Res. Lett., 35, L04808, doi:10.1029/2007GL032523, 2008.

Stier, P., Feichter, J., Kinne, S., Kloster, S., Vignati, E., Wilson, J., Ganzeveld, L., Tegen, I., Werner, M., Balkanski, Y., Schulz, M., Boucher, O., Minikin, A., and Petzold, A.: The aerosol-climate model ECHAM5-HAM, Atmos. Chem. Phys., 5, 1125–1156, doi:10.5194/acp-5-1125-2005, 2005.

Surratt, J. D., Kroll, J. H., Kleindienst, T. E., Edney, E. O., Claeys, M., Sorooshian, A., Ng, N. L., Offenberg, J. H., Lewandowski, M., Jaoui, M., Flagan, R. C., and Seinfeld, J. H.: Evidence for organosulfates in secondary organic aerosol, Environ. Sci. Technol., 41, 5363–5369, 2007.

Tsigaridis, K. and Kanakidou, M.: Secondary organic aerosol importance in the future atmosphere, Atmos. Environ., 41, 4682–4692, 2007.

Tsigaridis, K. and Kanakidou, M.: Global modelling of secondary organic aerosol in the troposphere: a sensitivity analysis, Atmos. Chem. Phys., 3, 1849–1869, doi:10.5194/acp-3-1849-2003, 2003.

Volkamer, R., Jimenez, J. L., San Martini, F., Dzepina, K., Zhang, Q., Salcedo, D., Molina, L. T., Worsnop, D. R., and Molina, M. J.: Secondary organic aerosol formation from anthropogenic air pollution: Rapid and higher than expected, Geophys. Res. Lett., 33, L17811, doi:10.1029/2006GL026899, 2006.

Volkamer, R., Ziemann, P. J., and Molina, M. J.: Secondary Organic Aerosol Formation from Acetylene (C_2H_2): seed effect on SOA yields due to organic photochemistry in the aerosol aqueous phase, Atmos. Chem. Phys., 9, 1907–1928, doi:10.5194/acp-9-1907-2009, 2009.

Wang, L., Khalizov, A. F., Zheng, J., Xu, W., Ma, Y., Lal, V., and Zhang, R.: Atmospheric nanoparticles formed from heterogenous reaction of organics, Nat. Geosci., 3, 238–242, 2010.

Yu, H., Kaufman, Y. J., Chin, M., Feingold, G., Remer, L. A., Anderson, T. L., Balkanski, Y., Bellouin, N., Boucher, O., Christopher, S., DeCola, P., Kahn, R., Koch, D., Loeb, N., Reddy, M. S., Schulz, M., Takemura, T., and Zhou, M.: A review of measurement-based assessments of the aerosol direct radiative effect and forcing, Atmos. Chem. Phys., 6, 613–666, doi:10.5194/acp-6-613-2006, 2006.